

1 **A common haplotype lowers PU.1 expression in myeloid cells and delays onset of**
2 **Alzheimer's disease**

3
4 Kuan-lin Huang^{1,2*}, Edoardo Marcora^{3,4*}, Anna A Pimenova⁴, Antonio F Di Narzo³, Manav
5 Kapoor^{3,4}, Sheng Chih Jin⁵, Oscar Harari⁶, Sarah Bertelsen⁴, Benjamin P Fairfax⁷, Jake
6 Czajkowski⁸, Vincent Chouraki⁹, Benjamin Grenier-Boley^{10,11,12}, Céline Bellenguez^{10,11,12},
7 Yuetiva Deming⁶, Andrew McKenzie³, Towfique Raj^{3,4}, Alan E Renton⁴, John Budde⁶, Albert
8 Smith¹³, Annette Fitzpatrick¹⁴, Joshua C Bis¹⁵, Anita DeStefano¹⁶, Hieab HH Adams¹⁷, M Arfan
9 Ikram¹⁷, Sven van der Lee¹⁷, Jorge L. Del-Aguila⁶, Maria Victoria Fernandez⁶, Laura Ibañez⁶,
10 The International Genomics of Alzheimer's Project¹⁸, The Alzheimer's Disease Neuroimaging
11 Initiative¹⁹, Rebecca Sims²⁰, Valentina Escott-Price²⁰, Richard Mayeux^{21,22,23}, Jonathan L
12 Haines²⁴, Lindsay A Farrer^{12,16,25,26,27}, Margaret A. Pericak-Vance^{27,28}, Jean Charles
13 Lambert^{10,11,12}, Cornelia van Duijn¹⁷, Lenore Launer²⁹, Sudha Seshadri⁹, Julie Williams²⁰,
14 Philippe Amouyel^{10,11,12,30}, Gerard D Schellenberg³¹, Bin Zhang³, Ingrid Borecki³², John S K
15 Kauwe³³, Carlos Cruchaga⁶, Ke Hao³, Alison M Goate^{3,4#}

16
17 ¹Department of Medicine, ²McDonnell Genome Institute, ⁶Department of Psychiatry,
18 ⁸Department of Genetics, Washington University in St. Louis, Saint Louis, MO, USA
19 ³Department of Genetics and Genomic Sciences, ⁴Ronald M. Loeb Center for Alzheimer's
20 disease, Department of Neuroscience, Icahn School of Medicine at Mount Sinai, New York, NY,
21 USA

22 ⁵Department of Genetics, Yale University School of Medicine, New Haven, CT, USA

23 ⁷Wellcome Trust Centre for Human Genetics, Nuffield Department of Medicine, University of
24 Oxford, Oxford, United Kingdom

25 ⁹Department of Neurology, ²⁵Department of Medicine (Biomedical Genetics), ²⁴Department of
26 Ophthalmology, Boston University School of Medicine, Boston, MA, USA

27 ¹⁰Inserm, U1167, RID-AGE –Risk factors and molecular determinants of aging-related diseases,
28 F-59000 Lille, France

29 ¹¹Univ. Lille - Excellence laboratory Labex DISTALZ, F-59000 Lille, France

30 ¹²Institut Pasteur de Lille, F-59000 Lille, France

31 ¹³University of Iceland, Reykjavik, Iceland

32 ¹⁴Department of Epidemiology, ¹⁵Department of Medicine, University of Washington, Seattle,
33 Washington, USA

34 ¹⁶Department of Biostatistics, ²⁶Department of Epidemiology, Boston University School of
35 Public Health, Boston, MA, USA

36 ¹⁷Department of Epidemiology, Erasmus University Medical Center, Rotterdam, The
37 Netherlands

38 ¹⁸Data used in the preparation of this article were obtained from the International Genomics of
39 Alzheimer's Project (IGAP), the investigators from which did not participate in the work
40 reported herein. IGAP authors and affiliations are documented in the 2013 landmark IGAP
41 publication¹.

42 ¹⁹Data used in preparation of this article were obtained from the Alzheimer's Disease
43 Neuroimaging Initiative (ADNI) database (adni.loni.usc.edu). As such, the investigators within
44 the ADNI contributed to the design and implementation of ADNI and/or provided data but did
45 not participate in analysis or writing of this report. A complete listing of ADNI investigators can
46 be found at:

47 http://adni.loni.usc.edu/wp-content/uploads/how_to_apply/ADNI_Acknowledgement_List.pdf

48

49 ²⁰Psychological Medicine and Clinical Neurosciences, Medical Research Council (MRC) Centre
50 for Neuropsychiatric Genetics and Genomics, Cardiff University, Cardiff, UK

51 ²¹Taub Institute on Alzheimer's Disease and the Aging Brain, ²²Gertrude H. Sergievsky Center,

52 ²³Department of Neurology, Columbia University, New York, NY, USA

53 ²⁴Department of Epidemiology and Biostatistics, Case Western Reserve University, Cleveland,
54 OH, USA

55 ²⁷The John P. Hussman Institute for Human Genomics, ²⁸Macdonald Foundation Department of
56 Human Genetics, University of Miami, Miami, FL, USA

57 ²⁹Laboratory of Epidemiology and Population Sciences, National Institute on Aging, Bethesda,
58 Maryland, USA

59 ³⁰Centre Hospitalier Universitaire de Lille, U1167, F-59000 Lille, France

60 ³¹Department of Pathology and Laboratory Medicine, University of Pennsylvania Perelman
61 School of Medicine, Philadelphia, PA, USA

62 ³²Regeneron Pharmaceuticals, Inc, NY, USA

63 ³³Department of Biology, Brigham Young University, Provo, Utah, USA

64

65

66

67

68 *These authors contributed equally to this work

69

70 #Corresponding Author:

71 Alison Goate, D.Phil.

72 Willard T.C. Johnson Research Professor of Neurogenetics

73 Director, Ronald M. Loeb Center for Alzheimer's disease

74 Dept. of Neuroscience, B1065

75 Icahn School of Medicine at Mount Sinai

76 1425 Madison Ave

77 New York, NY 10029

78 T: 212-659-5672

79 E-mail: alison.goate@mssm.edu

80

81

82 **Abstract**

83 A genome-wide survival analysis of 14,406 Alzheimer's disease (AD) cases and 25,849 controls
84 identified eight previously reported AD risk loci and fourteen novel loci associated with age at
85 onset. LD score regression of 220 cell types implicated regulation of myeloid gene expression in
86 AD risk. In particular, the minor allele of rs1057233 (G), within the previously
87 reported *CELF1* AD risk locus, showed association with delayed AD onset and lower expression
88 of *SPI1* in monocytes and macrophages. *SPI1* encodes PU.1, a transcription factor critical for
89 myeloid cell development and function. AD heritability is enriched within the PU.1 cistrome,
90 implicating a myeloid PU.1 target gene network in AD. Finally, experimentally altered PU.1
91 levels affect the expression of mouse orthologs of many AD risk genes and the phagocytic
92 activity of mouse microglial cells. Our results suggest that lower *SPI1* expression reduces AD
93 risk by regulating myeloid gene expression and cell function.

94
95

96 AD is the most prevalent form of dementia. While genome-wide association studies (GWAS)
97 have identified more than twenty AD risk loci¹⁻⁵, the associated disease genes and mechanisms
98 remain largely unclear. To better understand these genetic associations, AD-related phenotypes
99 can be leveraged. For example, few studies^{6,7} have investigated the genetic basis of age at onset
100 of AD (AAO). To date, *APOE* remains the only locus repeatedly associated with AAO^{8,9}, but
101 *PICALM* and *BINI* have also been reported to affect AAO^{6,10,11}. Further, we have previously
102 used CSF biomarkers to demonstrate that *APOE* genotype is strongly associated with these
103 disease-relevant endophenotypes^{12,13}.

104

105 Identifying causal genes and mechanisms underlying disease-associated loci requires integrative
106 analyses of expression and epigenetic datasets in disease-relevant cell types¹⁴. Recent genetic
107 and molecular evidence has highlighted the role of myeloid cells in AD pathogenesis. At the
108 genetic level, GWAS and sequencing studies have found associations between AD and genes
109 expressed in myeloid cells, including *TREM2*, *ABCA7*, and *CD33*^{1,2,5,15-17}. At the epigenetic level,
110 genes expressed in myeloid cells display abnormal patterns of chromatin modification in AD
111 mouse models and human samples¹⁸⁻²⁰. Further, AD-risk alleles are polarized for *cis*-expression
112 quantitative trait locus (*cis*-eQTL) effects in monocytes²¹. Herein, we show that AD heritability
113 is enriched in functional annotations for cells of the myeloid and B-lymphoid lineage, suggesting
114 that integrative analyses of AD loci with myeloid-specific expression and epigenetic datasets will
115 uncover novel AD genes and mechanisms related to the function of these cell types.

116

117 In this study, we conducted a large-scale genome-wide survival analysis and subsequent
118 endophenotype association analysis to uncover loci associated with AAO-defined survival
119 (AAOS) in AD cases and non-demented elderly controls. We discovered an AAOS- and CSF
120 A β ₄₂-associated SNP, rs1057233, in the previously reported *CELF1* AD risk locus. *Cis*-eQTL
121 analyses revealed a highly significant association of the protective rs1057233^G allele with
122 reduced *SPII* expression in human myeloid cells. *SPII* encodes PU.1, a transcription factor
123 critical for myeloid and B-lymphoid cell development and function, that binds to the *cis*-
124 regulatory elements of several AD-associated genes in these cells. Moreover, we show that AD
125 heritability is enriched in PU.1 ChIP-Seq binding sites in human myeloid cells across the
126 genome, implicating a myeloid PU.1 target gene network in the etiology of AD. To validate
127 these bioinformatic analyses, we show that experimentally altered PU.1 levels are correlated with
128 phagocytic activity of mouse microglial cells and the expression of multiple genes involved in
129 diverse biological processes of myeloid cells. This evidence collectively shows that lower *SPII*
130 expression may reduce AD risk by modulating myeloid cell gene expression and function.

131 Results

132

133 Genome-wide survival analysis

134 For the genome-wide survival analysis, we used 14,406 AD case and 25,849 control samples
135 from the IGAP consortium (**Table 1a**). 8,253,925 SNPs passed quality control and were included
136 for meta-analysis across all cohorts (**Supplementary Table 1**), which showed little evidence of
137 genomic inflation ($\lambda = 1.026$). Four loci showed genome-wide significant associations ($P < 5 \times 10^{-8}$)
138 with AAOS: *BINI* ($P=7.6 \times 10^{-13}$), *MS4A* ($P=5.1 \times 10^{-11}$), *PICALM* ($P=4.3 \times 10^{-14}$), and *APOE*
139 ($P=1.2 \times 10^{-67}$) (**Supplementary Fig. 1**). While SNPs within *BINI*⁶, *PICALM*^{6,10}, and *APOE*<sup>6,8-
140 10,22</sup> loci have previously been shown to be associated with AAO, this is the first time that the
141 *MS4A* locus is reported to be associated with an AAO-related phenotype. The minor allele of
142 rs7930318 near *MS4A4A* is associated with delayed AAO. Four other AD risk loci previously
143 reported in the IGAP GWAS¹ showed associations that reached suggestive significance ($P <$
144 1.0×10^{-5}): *CRI* ($P=1.2 \times 10^{-6}$), *SPII/CELF1* ($P=5.4 \times 10^{-6}$), *SORL1* ($P=1.8 \times 10^{-7}$), and *FERMT2*
145 ($P=1.0 \times 10^{-5}$). The direction of effects were concordant with the previous IGAP GWAS logistic
146 regression analysis for AD risk¹ at all suggestive loci: AD risk-increasing alleles were all
147 associated with a hazard ratio above 1 and earlier AAO, whereas AD risk-decreasing alleles were
148 all associated with a hazard ratio below 1 and later AAO (**Table 1b, Supplementary Table 2**).
149 We also identified 14 novel loci that reached suggestive significance in the survival analysis, 3 of
150 which (rs116341973, rs1625716, and rs11074412) were nominally associated with AD risk
151 (Bonferroni-corrected threshold: $P=0.05/22=2.27 \times 10^{-3}$) in the IGAP GWAS (**Table 1b,**
152 **Supplementary Fig. 2, 3**).

153

154 Cerebrospinal fluid biomarkers associations

155

156 To further validate the 22 loci with at least suggestive associations to AAOS, we examined their
157 associations with CSF biomarkers, including total tau, phosphorylated tau₁₈₁, and A β ₄₂ in a
158 dataset of 3,646 Caucasians extended from our previous report¹² (**Table 2**). Two SNPs showed
159 associations that reached the Bonferroni-corrected threshold ($P < 2.27 \times 10^{-3}$). Rs4803758 near
160 *APOE* showed the most significant associations with levels of CSF phosphorylated tau₁₈₁
161 ($P=3.75 \times 10^{-4}$) and CSF A β ₄₂ ($P=3.12 \times 10^{-5}$), whereas rs1057233 in the *SPII/CELF1* locus was
162 significantly associated with CSF A β ₄₂ ($P=8.24 \times 10^{-4}$). Of note, a SNP adjacent to *VLDLR*,
163 rs7867518, showed the most significant association with CSF total tau ($P=3.02 \times 10^{-3}$), but failed
164 to pass the Bonferroni-corrected threshold. The protective and deleterious effects in the survival
165 analysis of these three SNPs were concordant with directionalities of their CSF biomarker
166 associations; for example, the protective rs1057233^G allele was associated with higher CSF A β ₄₂
167 levels and the risk rs1057233^A allele was associated with lower CSF A β ₄₂ levels.

168

169 Cis-eQTL associations and colocalization analysis

170

171 Multiple disease-associated GWAS SNPs have been identified as *cis*-eQTLs of disease genes in
172 disease-relevant tissues/cell types²³. We investigated *cis*-eQTL effects of the 22 AAOS-
173 associated SNPs and their tagging SNPs ($R^2 \geq 0.8$, listed in **Supplementary Table 3**) in the
174 BRAINEAC dataset. We identified 4 significant associations (Bonferroni-corrected threshold:
175 $P=0.05/292,000$ probes = 1.7×10^{-7}): rs1057233 was associated with *MTCH2* expression in the
176 cerebellum ($P=1.20 \times 10^{-9}$); rs7445192 was associated with *SRA1* expression averaged across

177 brain regions ($P=7.0\times 10^{-9}$, 1.6×10^{-7} for two probes respectively), and rs2093761 was associated
178 with *CR1/CRIL* expression in white matter ($P=1.30\times 10^{-7}$, **Supplementary Table 4**). Further
179 analysis using the GTEx dataset²⁴ identified 50 unique, associated snp-gene pairs across 44
180 tissues, including 11 snp-gene pairs in various brain regions (**Supplementary Table 5**).

181
182 Recently, genetic and molecular evidence has implicated myeloid cells in the etiology of AD,
183 including our finding that AD risk alleles are enriched for *cis*-eQTL effects in monocytes but not
184 CD4+ T-lymphocytes²¹. To extend this finding and identify relevant cell types in AD, we used
185 stratified LD score regression to estimate enrichment of AD heritability (measured by summary
186 statistics from IGAP GWAS¹) partitioned by 220 cell type-specific functional annotations as
187 described by Finucane et al.²⁵. We found a significant enrichment of AD heritability in
188 hematopoietic cells of the myeloid and B-lymphoid lineage (e.g., 14.49 fold enrichment,
189 $P=3.49\times 10^{-5}$ in monocytes/CD14 enhancers/H3K4me1 and 12.33 fold enrichment, $P=1.41\times 10^{-6}$
190 in B-cells/CD19 enhancers/H3K4me1). In contrast schizophrenia (SCZ) heritability was not
191 enriched in hematopoietic cells (1.24 fold enrichment, $P=0.53$, as measured by summary
192 statistics from the Psychiatric Genomics Consortium [PGC] GWAS²⁶) but was significantly
193 enriched in brain (18.61 fold enrichment, $P=1.38\times 10^{-4}$ in fetal brain promoters/H3K4me3,
194 **Supplementary Table 6**). These results suggest that myeloid cells specifically modulate AD
195 susceptibility.

196
197 Based on these observations, we hypothesized that *cis*-eQTL effects of some AD-associated
198 alleles may be specific to myeloid cells and thus not easily detectable in *cis*-eQTL datasets
199 obtained from brain homogenates where myeloid cells (microglia and other brain-resident
200 macrophages) represent a minor fraction of the tissue. Therefore, we analyzed *cis*-eQTL effects
201 of the AAOS-associated SNPs and their tagging SNPs in human *cis*-eQTL datasets composed of
202 738 monocyte and 593 macrophage samples from the Cardiogenics consortium²⁷. We identified
203 14 genes with *cis*-eQTLs significantly associated with these SNPs (**Table 3**). Notably, the
204 protective rs1057233^G allele, located within the 3' UTR of *SPII*, was strongly associated with
205 lower expression of *SPII* in both monocytes ($P=1.50\times 10^{-105}$) and macrophages ($P=6.41\times 10^{-87}$)
206 (**Fig. 1a, 1b, 2a**). This allele was also associated with lower expression of *MYBPC3* (monocytes:
207 $P=5.58\times 10^{-23}$; macrophages: $P=4.99\times 10^{-51}$), higher expression of *CELF1* in monocytes
208 ($P=3.95\times 10^{-8}$) and lower *NUP160* expression in macrophages ($P=5.35\times 10^{-22}$). Each of these
209 genes lies within the *SPII/CELF1* locus, suggesting complex regulation of gene expression in
210 this region. Within the *MS4A* locus, which contains many gene family members, the minor allele
211 (C) of rs7930318 was consistently associated with lower expression of *MS4A4A* in monocytes
212 ($P=8.20\times 10^{-28}$) and *MS4A6A* in monocytes ($P=4.90\times 10^{-23}$) and macrophages ($P=1.25\times 10^{-9}$, **Fig.**
213 **1b**). Among the novel AAOS-associated loci, rs5750677 was significantly associated with lower
214 expression of *SUN2* in both monocytes ($P=3.66\times 10^{-58}$) and macrophages ($P=3.15\times 10^{-36}$),
215 rs10919252 was associated with lower expression of *SELL* in monocytes ($P=7.33\times 10^{-35}$), and
216 rs1625716 was associated with lower expression of *CISDI* in macrophages ($P=5.98\times 10^{-23}$, **Table**
217 **3**).

218
219 We then sought evidence of replication in an independent dataset of primary CD14+ human
220 monocytes from 432 individuals²⁸. We replicated *cis*-eQTL associations with expression of *SPII*,
221 *MYBPC3*, *MS4A4A*, *MS4A6A*, and *SELL* (Bonferroni-corrected threshold: $P=0.05/15421$ probes
222 = 3.24×10^{-6}). We found strong evidence for the association between rs1057233 and *SPII*

223 expression ($P=6.39 \times 10^{-102}$) as well as *MYBPC3* expression ($P=5.95 \times 10^{-33}$, **Supplementary**
224 **Table 7**). Rs1530914 and rs7929589, both in high LD with rs7930318 ($R^2 = 0.99$ and 0.87 ,
225 respectively), were associated with expression of *MS4A4A* and *MS4A6A* ($P=3.60 \times 10^{-8}$, 6.37×10^{-15}),
226 respectively. Finally, rs2272918, tagging rs10919252, was significantly associated with
227 expression of *SELL* ($P=8.43 \times 10^{-16}$). Interestingly, the minor allele of all of these SNPs showed
228 protective effects in both AD risk and survival analyses, as well as lower expression of the
229 associated genes. Further, *SPII*, *MS4A4A*, *MS4A6A*, and *SELL* are specifically expressed in
230 microglia based on RNA-Seq data²⁹⁻³¹ (**Fig. 2b**, **Supplementary Fig. 4**). However,
231 *MYBPC3/Mybpc3* (a myosin binding protein expressed at high levels in cardiac muscle cells) is
232 either not expressed or expressed at low levels in human and mouse microglia, respectively.
233 Amongst all genes probed, *MYBPC3* (ILMN_1781184) expression is the most highly and
234 significantly correlated with *SPII* (ILMN_1696463) expression in both Cardiogenics datasets
235 (Spearman's rho = 0.54, qval = 0.00 in monocytes and Spearman's rho = 0.42, qval = 0.00 in
236 macrophages) suggesting that low levels of *MYBPC3* expression in human myeloid cells are
237 possibly due to leaky transcription driven by the adjacent highly expressed *SPII* gene.

238
239 We performed the coloc test³² to determine whether AAOS-associated SNPs co-localize with
240 myeloid *cis*-eQTLs at the *SPII/CELF1*, *MS4A* and *SELL* loci. These analyses (**Supplementary**
241 **Table 8**) highlighted *SPII* at the *SPII/CELF1* locus as the strongest and most consistent
242 colocalization target, and the only gene where the AD survival and gene expression association
243 signals are likely (posterior probability ≥ 0.8) driven by the same causal genetic variant, in both
244 monocytes and macrophages (PP.H4.abf of 0.85 and 0.83, respectively). *MYBPC3* in the
245 *SPII/CELF1* locus and *MS4A6A* in the *MS4A* locus also showed evidence of colocalization in
246 both myeloid cell types albeit not surviving posterior probability cutoff in one of them. *MS4A4A*
247 and *MS4A6E* in the *MS4A* locus showed evidence of co-localization only in monocytes, while
248 *SELL* did not show evidence of colocalization.

249
250 In light of the strong *cis*-eQTL effects and colocalization results described above, we decided to
251 focus subsequent analyses on *SPII* as the strongest candidate gene underlying the disease
252 association in myeloid cells.

253 254 **Conditional and SMR analysis of the *SPII/CELF1* locus**

255
256 The AAOS-association landscape shows that highly associated SNPs at the *SPII/CELF1* locus
257 span multiple genes (**Fig. 1a**). In the previous IGAP GWAS¹, rs10838725 showed the strongest
258 association at this locus ($P=6.7 \times 10^{-6}$, 1.1×10^{-8} vs. rs1057233: $P=5.4 \times 10^{-6}$, 5.9×10^{-7} in IGAP stage
259 I, stage I and II combined, respectively). Rs10838725 is located in the intron of *CELF1*, which
260 was assigned as the putative causal gene at this locus¹ based on proximity to the index SNP, a
261 criterion that has often proven to be erroneous¹⁴. In our survival analysis, however, rs10838725
262 showed weak association ($P=0.12$, HR=1.02, 95% CI=0.99-1.05) whereas rs1057233, located in
263 the 3'UTR of a neighboring gene, *SPII*, showed the strongest association (**Table 1**, $P=5.4 \times 10^{-6}$).
264 The two SNPs exhibit only moderate linkage disequilibrium in the ADGC subset of the IGAP
265 GWAS ($R^2=0.21$, $D'=0.96$). Applying conditional logistic regression analysis of AD risk in the
266 ADGC dataset, we found that rs1057233 remained significantly associated with AD after
267 adjusting for rs10838725 ($P=3.2 \times 10^{-4}$), whereas rs10838725 showed no evidence of association

268 after adjusting for rs1057233 ($P=0.66$). This suggests that rs1057233 is in stronger LD with the
269 AD risk causal variant.

270
271 The association landscape in the AD survival analysis highly resembles that of *SPII* *cis*-eQTL
272 analysis in myeloid cells (**Fig. 1a**). We reasoned that the associations of rs1057233 with AD-
273 related phenotypes may be explained by the regulation of *SPII* expression in myeloid cells, and
274 that conditional analysis of the *cis*-eQTL signal could help us further dissect this complex locus.
275 Therefore, we conducted conditional *cis*-eQTL analyses in both Cardiogenics datasets as we did
276 above using rs1057233 (the top SNP for AD survival) and rs10838725 (the top SNP for AD risk).
277 In addition, we also examined rs10838698 (a SNP in high LD with rs1057233 that was directly
278 genotyped in the Cardiogenics dataset) and rs1377416, a SNP in high LD with rs10838725
279 proposed to be a functional variant in an enhancer near *SPII* that is active in human myeloid
280 cells and in the brain of a mouse model of AD¹⁹. It should be noted that rs1057233 is a functional
281 variant that has been shown to directly affect *SPII* expression by changing the target sequence
282 and binding of miR-569³³. Rs1057233 and rs10838698 remained significantly associated with
283 *SPII* expression when adjusting for either of the other two SNPs in both monocytes and
284 macrophages ($P < 8.33 \times 10^{-3}$). However, conditioning for either of these two SNPs abolished the
285 associations of rs1377416 and rs10838725 with *SPII* expression (**Supplementary Table 9**).
286 Thus, the functional variant(s) mediating the effect on *SPII* expression and AD risk likely
287 reside(s) in the LD block that includes rs1057233 and rs10838698 but not rs10838725 and
288 rs1377416 (**Supplementary Fig. 5**).

289
290 Using HaploReg³⁴ to annotate the top AAOS-associated SNP (rs1057233) and its tagging SNPs
291 ($R^2 \geq 0.8$, **Supplementary Table 3**), we identified multiple SNPs (e.g. rs10838699 and
292 rs7928163) in tight LD with rs1057233 that changed the predicted DNA binding motif of SPI1
293 (PU.1), raising the possibility of altered self-regulation associated with the minor allele. Based
294 on these results, one or more of these or other SNPs in very high LD with rs1057233, could
295 explain the observed associations with *SPII* expression and AD-related phenotypes.

296
297 We also conducted Summary-data-based Mendelian Randomization (SMR) and Heterogeneity In
298 Dependent Instruments (HEIDI) tests²³ to prioritize likely causal genes and variants by
299 integrating summary statistics from our AAOS GWAS and the Cardiogenics study
300 (**Supplementary Table 10**). SMR/HEIDI analysis was performed for the *SPII/CELF1* locus
301 using rs1057233, rs10838698, rs10838699, rs7928163, rs10838725 and rs1377416 as candidate
302 causal variants. In both monocytes and macrophages, *SPII* was consistently identified as the
303 most likely gene whose expression levels are associated with AD survival because of
304 causality/pleiotropy at the same underlying causal variant (rs1057233, rs10838698, rs10838699,
305 or rs7928163 in the same LD block) (SMR $P < 4.90 \times 10^{-4}$, Bonferroni-corrected threshold for 6
306 SNPs tested against 17 probes and HEIDI $P \geq 0.05$, **Supplementary Fig. 6**). Neither conditional
307 analysis nor SMR/HEIDI analysis could definitively identify a single functional variant among
308 this set of 4 SNPs in high LD. Functional analyses will be necessary to determine which SNPs in
309 this LD block directly affects *SPII* expression. Overall, rs1057233 and tagging SNPs are
310 associated with AD risk and survival, and CSF $A\beta_{42}$. The strong *cis*-eQTL effects and
311 colocalization results point to *SPII* as the most likely candidate gene underlying the disease
312 association at the *SPII/CELF1* locus.

313

314

315 **SPI1 (PU.1) cistrome and functional analysis in myeloid cells**

316

317 *SPI1* encodes PU.1, a transcription factor essential for the development and function of myeloid
318 cells. We hypothesize that it may modulate AD risk by regulating the transcription of AD-
319 associated genes expressed in microglia and/or other myeloid cell types. First, we tested AD-
320 associated genes for evidence of expression in human microglia²⁹ as well as presence of PU.1
321 binding peaks in *cis*-regulatory elements of these genes using ChIP-Seq datasets obtained from
322 human monocytes and macrophages³⁵. We specifically investigated 112 AD-associated genes,
323 including the 104 genes located within IGAP GWAS loci³⁶ and *APOE*, *APP*, *TREM2* and
324 *TREML2*, *TYROBP*, *TRIP4*, *CD33*, and *PLD3*. Among these genes, 75 had evidence of gene
325 expression in human brain microglial cells, 60 of which also had evidence of association with
326 PU.1 binding sites in human blood myeloid cells³⁵ (**Supplementary Table 11**). Further
327 examination of PU.1 binding peaks and chromatin marks/states in human monocytes confirmed
328 that PU.1 is bound to *cis*-regulatory elements of many AD-associated genes, including *ABCA7*,
329 *CD33*, *MS4A4A*, *MS4A6A*, *PILRA*, *PILRB*, *TREM2*, *TREML2*, and *TYROBP* (as well as *SPI1*
330 itself, but notably not *APOE*) (**Fig. 2c, Supplementary Fig. 7**). Together, these results suggest
331 that PU.1 may regulate the expression of multiple AD-associated genes in myeloid cells.

332

333 To further support that PU.1 target genes expressed in myeloid cells may be associated with AD
334 risk, we used stratified LD score regression²⁵ to estimate enrichment of AD heritability (as
335 measured by summary statistics from the IGAP GWAS¹) partitioned on the PU.1 cistrome, as
336 profiled by ChIP-Seq in human monocytes and macrophages³⁵. We found a significant
337 enrichment of AD heritability in both monocytes (47.58 fold enrichment, $P=6.94 \times 10^{-3}$) and
338 macrophages (53.88 fold enrichment, $P=1.65 \times 10^{-3}$), but not SCZ heritability [as measured by
339 summary statistics from the PGC GWAS²⁶] (**Supplementary Table 12**). Thus, the contribution
340 of the myeloid PU.1 target gene network to disease susceptibility is specific to AD. However,
341 since PU.1 is a key myeloid transcription factor that regulates the expression of a large number
342 of genes in myeloid cells, the enrichment of AD risk alleles in PU.1 binding sites could simply
343 reflect an enrichment of AD GWAS associations for genes that are expressed in myeloid cells
344 rather than specifically among PU.1 target genes. To attempt to address this issue, we performed
345 stratified LD score regression of AD heritability partitioned by functional annotations obtained
346 from *SPI1* (marking the PU.1 cistrome) and POLR2AphosphoS5 (marking actively transcribed
347 genes) ChIP-Seq experiments, performed in duplicate, using a human myeloid cell line (HL60)
348 by the ENCODE Consortium³⁷. We observed a significant enrichment for *SPI1* (PU.1) (34.58
349 fold enrichment, $P=1.31 \times 10^{-3}$ in first replicate; 58.12 fold enrichment, $P=4.95 \times 10^{-3}$ in second
350 replicate) much stronger than that for POLR2AphosphoS5 (15.78 fold enrichment, $P=1.71 \times 10^{-2}$
351 in first replicate; 16.34 fold enrichment, $P=1.25 \times 10^{-1}$ in second replicate), consistent with our
352 hypothesis (**Supplementary Table 12**).

353

354 PU.1 target genes are implicated in various biological processes of myeloid cells that may
355 modulate AD risk. For example, a microglial gene network for pathogen phagocytosis has been
356 previously implicated in the etiology of AD¹⁸. We modulated levels of PU.1 by *Spi1* cDNA
357 overexpression or shRNA knock-down in BV2 mouse microglial cells, and used zymosan
358 bioparticles labeled with pHrodo (a pH-sensitive dye that emits a fluorescent signal when
359 internalized in acidic vesicles during phagocytosis) to measure pathogen engulfment. Analysis of

360 zymosan uptake by flow cytometry revealed that phagocytic activity is augmented in BV2 cells
361 overexpressing PU.1 (**Fig. 3a**), while knock-down of PU.1 resulted in decreased phagocytic
362 activity (**Fig. 3a**). We confirmed overexpression and knock-down of PU.1 expression levels by
363 western blotting and qPCR (**Fig. 3**). Phagocytic activity was not changed in untransfected cells
364 when analyzed by flow cytometry (**Supplementary Fig. 8d, 8e, 8f, 8g**). These data suggest that
365 modulation of PU.1 expression levels significant changes microglial phagocytic activity in
366 response to fungal targets (mimicked by zymosan).

367
368 To further explore the functional impact of variation in *SP11* expression, we performed qPCR to
369 test whether differential *Spi1* expression in BV2 cells can modulate expression of genes thought
370 to play important roles in AD pathogenesis and/or microglial cell function (**Fig. 3**,
371 **Supplementary Fig. 9, Supplementary Table 13, 14**). We found that levels of some of these
372 genes were affected in opposing directions by overexpression and knock-down of *Spi1* (**Fig. 4a**),
373 while other genes were affected only by overexpression (**Fig. 4b**) or knock-down (**Fig. 4c**) or not
374 affected at all (**Supplementary Fig. 9**). After knock-down of *Spi1* in BV2 cells, expression of
375 *Cd33*, *Tyrobp*, *Ms4a4a* and *Ms4a6d* decreased and expression of *ApoE* and *Clu/ApoJ* increased
376 (**Fig. 4a, 4c**). These data demonstrate that multiple microglial genes, some already implicated in
377 AD, are selectively perturbed by altered expression of *Spi1*.

378 Discussion

379
380 By performing a large-scale genome-wide survival analysis, we discovered multiple loci
381 associated with AAOS (**Table 1**). The four genome-wide significantly associated loci, *BIN1*
382 ($P=7.6 \times 10^{-13}$), *MS4A* ($P=5.1 \times 10^{-11}$), *PICALM* ($P=4.3 \times 10^{-14}$), and *APOE* ($P=1.2 \times 10^{-67}$), have been
383 previously reported to be associated with AD risk¹. Notably, this is the first study showing that
384 the *MS4A* locus is associated with AAOS. The most significantly AAOS-associated SNP at this
385 locus, rs7930318, shows a protective effect (HR = 0.93, 95% CI = 0.90-.95) in the survival
386 analysis, consistent with the previous IGAP GWAS logistic regression analysis for AD risk (OR
387 = 0.90, 95% CI = 0.87-.93).

388
389 By combining AAOS and CSF biomarker GWAS results, we provide evidence of AD
390 association at additional loci (**Table 2**). In particular, rs7867518 at the *VLDLR* locus shows
391 suggestive associations with both AAOS ($P=9.1 \times 10^{-6}$) and CSF tau ($P=3.03 \times 10^{-3}$). An adjacent
392 SNP (rs2034764) in the neighboring gene, *KCNV2*, has been previously reported to have
393 suggestive association with AAO²². *VLDLR* is a receptor for lipoproteins containing APOE³⁸
394 and *CLU/APOJ*³⁹, another AD risk gene. Additionally, the *VLDLR*-5-repeat allele was found to
395 be associated with dementia³⁸. This genetic and biochemical evidence suggests *VLDLR* may be
396 linked to AD.

397
398
399 *Cis*-eQTL analyses of AAOS-associated SNPs revealed limited associations when using data
400 from brain tissue homogenates, yet identified multiple candidate genes when using data from
401 myeloid cells, the top candidate causal cell types for AD based on the stratified LD score
402 regression analysis of AD heritability presented here. This calls attention to careful selection of
403 relevant cell types in eQTL studies of disease associations. In particular, by conducting *cis*-eQTL
404 analyses using monocyte and macrophage datasets, we discovered associations of AAOS-
405 associated SNPs with the expression of *SELL*, *SP11*, *MYBPC3*, *NUP160*, *MS4A4A*, *MS4A6A* and

406 *SUN2* (**Table 3**). Furthermore, we replicated the *cis*-eQTL associations of rs1057233 with *SP11*,
407 *MYBPC3*, rs7930318 with *MS4A4A*, *MS4A6A* and rs2272918 with *SELL* in an independent
408 monocyte dataset. We further showed that *SP11* myeloid *cis*-eQTLs and AAOs-associated SNPs
409 are not likely to be colocalized by chance and thus may be in the causal path to AD (**Fig. 1**).
410 Notably, the minor allele of rs1057233 (G) is suggestively associated with lower AD risk
411 ($P=5.4 \times 10^{-6}$, 5.9×10^{-7} in IGAP stage I, stage I and II combined, respectively)¹, later AAO
412 ($P=8.4 \times 10^{-6}$) and significantly associated with higher CSF A β_{42} ($P=4.11 \times 10^{-4}$), which likely
413 reflects decreased A β aggregation and β -amyloid deposition in the brain. Furthermore, it is
414 strongly associated with lower *SP11* expression in human monocytes ($P=1.50 \times 10^{-105}$) and
415 macrophages ($P=6.41 \times 10^{-87}$, **Table 3**).

416
417 Colocalization analyses using coloc³² and SMR/HEIDI²³ support the hypothesis that the same
418 causal SNP(s) influence *SP11* expression and AD risk. However, neither conditional nor
419 SMR/HEIDI analyses were able to pin-point an individual SNP; both approaches identified an
420 LD block tagged by rs1057233, in which one or more SNPs may individually or in combination
421 influence both *SP11* expression and AD risk. rs1057233 changes the target sequence and binding
422 of miR-569³³, and its tagging SNPs alter binding motifs of transcription factors including PU.1
423 itself (**Supplementary Table 3 and Supplementary Fig. 7d**). rs1377416, is located in a
424 predicted enhancer in the vicinity of *SP11* and altered enhancer activity when assayed *in vitro*
425 using a reporter construct transfected in BV2 cells¹⁹. However, rs1057233 remained significantly
426 associated with AD after conditioning for either rs1377416 ($P=1.2 \times 10^{-3}$) or the previously
427 reported IGAP GWAS top SNP rs10838725 ($P=3.2 \times 10^{-4}$) in the ADGC dataset. Further, the *cis*-
428 eQTL association between rs1057233 and *SP11* expression remained significant after
429 conditioning for either of these SNPs, whereas conditioning for rs1057233 abolished their *cis*-
430 eQTL associations with *SP11* (**Supplementary Table 9**). Thus, rs1057233 and its tagging SNPs
431 likely represent the underlying disease locus and may modulate AD risk through variation in
432 *SP11* expression. Interestingly, rs1057233 was previously found to be associated with systemic
433 lupus erythematosus³³, body mass index⁴⁰ and proinsulin levels⁴¹ and may contribute to the
434 connection between AD, immune cell dysfunction, obesity and diabetes.

435
436 PU.1 binds to *cis*-regulatory elements of several AD-associated genes expressed in human
437 myeloid cells, including *ABCA7*, *CD33*, *MS4A4A*, *MS4A6A*, *TREM2*, and *TYROBP* (**Fig. 1e**,
438 **Supplementary Fig. 7**). Further, PU.1 binds to active enhancers of *Trem2* and *Tyrobp* in ChIP-
439 Seq experiments using mouse BV2 cells⁴² or bone marrow-derived mouse macrophages⁴³. PU.1
440 is required for the development and function of myeloid and B-lymphoid cells^{44,45}. In particular,
441 PU.1 expression is dynamically and tightly controlled during haematopoiesis to direct the
442 specification of CD34+ hematopoietic stem and progenitor cells toward the myeloid and B-
443 lymphoid lineage by progressively partitioning into CD14+ monocytes/macrophages, CD15+
444 neutrophils, and CD19+ B cells⁴⁶, which are the cell types highlighted by our stratified LD score
445 regression analysis. Given its selective expression in microglia in the brain (**Fig. 2b**), PU.1 may
446 modify microglial cell function through transcriptional regulation of target genes that act as
447 downstream modulators of AD susceptibility, as evidenced by the significant enrichment of AD
448 heritability partitioned on the PU.1 cistrome in human myeloid cells (**Supplementary Table 12**).

449
450 In support of this hypothesis, we also demonstrate that changes in PU.1 expression levels alter
451 phagocytic activity in BV2 mouse microglial cells (**Fig. 3, Supplementary Fig. 8**). Knock-down

452 of PU.1 expression reduced engulfment of zymosan, whereas overexpression of PU.1 increased
453 engulfment of zymosan, a Toll-like receptor 2 (TLR2) agonist that mimics fungal pathogens.
454 This is in line with previous data showing decreased uptake of A β ₄₂ (also a TLR2 agonist) in
455 primary microglial cells isolated from adult human brain tissue and transfected with siRNA
456 targeting *SPI1*⁴⁷. Interestingly, several AD-associated genes (e.g., *CD33*, *TYROBP*, *TREM2*,
457 *TREML2*, *CR1*, *ABCA7*, *APOE*, *CLU/APOJ*) have been shown to be involved in the phagocytic
458 clearance of pathogens or host-derived cellular material (e.g., β -amyloid, apoptotic cells, myelin
459 debris, lipoproteins, etc.), suggesting a strong link between perturbation of microglial
460 phagocytosis and AD pathogenesis. In addition to *Cd33*, *Tyrobp*, *ApoE* and *Clu/ApoJ*, several
461 genes with roles in phagocytosis are dysregulated by altering *Spi1* expression, i.e. *Cd36*, *Fcgr1*,
462 *P2ry12*, *Itgam*, *Cx3cr1*, *Axl*, *Ctsb* (**Fig. 4a, 4b, 4c**), suggesting a collective and coordinated effect
463 of *Spi1* on the phagocytic activity of BV2 cells.

464
465 Our genetic analyses show that the protective allele at the *MS4A* locus is associated with lower
466 expression of *MS4A4A* and *MS4A6A* in human myeloid cells, and the BV2 experiment
467 demonstrated that lower expression of *Spi1* (which is protective in humans) led to lower
468 expression of *Ms4a4a* and *Ms4a6d* (mouse ortholog of *MS4A6A*), which are also associated with
469 reduced AD risk in humans. Transcriptomic and proteomic analyses of microglial cells suggested
470 a microglial homeostatic signature that is perturbed during aging and under pathological
471 conditions⁴⁸. It will be valuable to test whether genetically altered *SPI1* levels prime microglia to
472 exacerbate or alleviate transcriptional responses that occur during aging or disease development.
473 Together with genetic variation in myeloid genes associated with AD as an amplifier, *SPI1* may
474 be a master regulator capable of tipping the balance toward a neuroprotective or neurotoxic
475 microglial phenotype.

476
477 PU.1 expression levels regulate multiple myeloid/microglial cell functions⁴⁷, including
478 proliferation, survival and differentiation, that could also modulate AD risk. Indeed, expression
479 of *Il34* and *Csf1*, soluble factors that bind to *Csf1r* and required for microglial development and
480 maintenance *in vivo*⁴⁹, were elevated after knock-down of *Spi1*, while expression of *Csf1r* was
481 reduced (**Fig. 4a, 4c**). Interestingly, inhibition of *Csf1r* in a 3xTg-AD mouse model led to a
482 reduction in the number of microglia associated with β -amyloid plaques and improved
483 cognition⁵⁰. These findings suggest the importance of analyzing cell proliferation, survival,
484 differentiation, and migration phenotypes with differential *Spi1* expression, because *Spi1* levels
485 modulate expression of *Ccl2* and *Cxcl2* (**Fig. 4a**), which are MCP1 and MIP2 α proteins that help
486 recruit circulating monocytes and neutrophils to the brain to promote neuroinflammation. In
487 addition, knocking down *Spi1* reduced expression of a microgliosis marker *Aif1* (*Iba1*) along
488 with *Il1b*, *Nos2*, *Ptgs2*, *Arg1* and *Nlrp3* (**Fig. 4a, 4c**), suggesting that decreased *Spi1* expression
489 may blunt the pro-inflammatory response of microglial cells to improve disease outcomes.
490 Interestingly, expression of *Cx3cr1* and *Axl* were elevated upon knock-down of *Spi1* (**Fig. 4c**),
491 raising the possibility that beneficial effects of changes in *Spi1* expression are exerted through
492 modulation of synaptic or neuronal clearance. Further experimental investigation of these
493 phenotypes may shed light on the mechanisms of *SPI1* modulation of AD risk. Of note,
494 overexpression and knock-down of *Spi1* in BV2 cells produce different and often opposite
495 changes in expression of the genes profiled here, possibly driving alternative phenotypes that
496 may underlie detrimental and protective roles of PU.1.

497

498 In summary, by combining AD survival and endophenotype GWAS analyses, we replicated and
499 discovered multiple genetic loci associated with AAOAOS. Specifically, we nominate *SPII* as
500 the gene responsible for disease association at the previously reported *CELF1* locus. *SPII*
501 encodes PU.1, a transcription factor expressed in microglia and other myeloid cells that directly
502 regulates other AD-associated genes expressed in these cell types. Our data suggest that lower
503 *SPII* expression reduces risk for AD, suggesting a novel therapeutic approach to the treatment of
504 AD. Furthermore, we demonstrate that AAOS-associated SNPs within the *MS4A* gene cluster
505 are associated with eQTLs in myeloid cells for both *MS4A4A* and *MS4A6A*. Specifically, the
506 allele associated with reduced AD risk is associated with lower *MS4A4A* and *MS4A6A*
507 expression. This is consistent with the observation that lowering *SPII* expression, which is
508 protective for AD risk, also lowers *MS4A4A* and *MS4A6A* expression. These results reinforce the
509 emerging genetic and epigenetic association between AD and a network of microglial expressed
510 genes^{2,5,17-21}, highlighting the need to dissect their functional mechanisms.
511
512

513 **Acknowledgements**

514 We would like to thank the patients, control subjects, and their family members for participating
515 in or supporting the research projects included in this study. We thank Marc Diamond (UT
516 Southwestern Medical Center) for the BV2 cell line and Flow Cytometry CORE at the Icahn
517 School of Medicine at Mount Sinai Hospital.

518 **IGAP**

519 GERAD was supported by the Wellcome Trust, the MRC, Alzheimer's Research UK (ARUK)
520 and the Welsh government. ADGC and CHARGE were supported by the US National Institutes
521 of Health, National Institute on Aging (NIH-NIA), including grants U01 AG032984 and R01
522 AG033193. CHARGE was also supported by Erasmus Medical Center and Erasmus University.

523 **ADNI**

524 Data collection and sharing for this project was funded by the Alzheimer's Disease
525 Neuroimaging Initiative (ADNI) (National Institutes of Health Grant U01 AG024904) and DOD
526 ADNI (Department of Defense award number W81XWH-12-2-0012). ADNI is funded by the
527 National Institute on Aging, the National Institute of Biomedical Imaging and Bioengineering,
528 and through generous contributions from the following: AbbVie, Alzheimer's Association;
529 Alzheimer's Drug Discovery Foundation; Araclon Biotech; BioClinica, Inc.; Biogen; Bristol-
530 Myers Squibb Company; CereSpir, Inc.; Eisai Inc.; Elan Pharmaceuticals, Inc.; Eli Lilly and
531 Company; EuroImmun; F. Hoffmann-La Roche Ltd and its affiliated company Genentech, Inc.;
532 Fujirebio; GE Healthcare; IXICO Ltd.; Janssen Alzheimer Immunotherapy Research &
533 Development, LLC.; Johnson & Johnson Pharmaceutical Research & Development LLC.;
534 Lumosity; Lundbeck; Merck & Co., Inc.; Meso Scale Diagnostics, LLC.; NeuroRx Research;
535 Neurotrack Technologies; Novartis Pharmaceuticals Corporation; Pfizer Inc.; Piramal Imaging;
536 Servier; Takeda Pharmaceutical Company; and Transition Therapeutics. The Canadian Institutes
537 of Health Research is providing funds to support ADNI clinical sites in Canada. Private sector
538 contributions are facilitated by the Foundation for the National Institutes of Health
539 (www.fnih.org). The grantee organization is the Northern California Institute for Research and
540 Education, and the study is coordinated by the Alzheimer's Disease Cooperative Study at the
541 University of California, San Diego. ADNI data are disseminated by the Laboratory for Neuro
542 Imaging at the University of Southern California

543
544 We thank the Cardiogenics (European Project reference LSHM-CT-2006-037593) project for
545 providing summary statistics for the *cis*-eQTL-based analyses. We also thank the ENCODE
546 Consortium and Richard Myers' lab (HAIB) for providing ChIP-Seq datasets.

547
548 This work was supported by grants from the National Institutes of Health (U01 AG049508
549 (AMG), R01-AG044546 (CC), RF1AG053303 (CC) and R01-AG035083 (AMG), RF-
550 AG054011 (AMG)), the JPB Foundation (AMG) and FBRI (AMG). The recruitment and clinical
551 characterization of research participants at Washington University were supported by NIH P50
552 AG05681, P01 AG03991, and P01 AG026276. Kuan-lin Huang received fellowship funding in
553 part from the Ministry of Education in Taiwan and the Lucille P. Markey Special Emphasis
554 Pathway in Human Pathobiology. Ke Hao is partially supported by the National Natural Science
555 Foundation of China (Grant No. 21477087, 91643201) and by the Ministry of Science and
556 Technology of China (Grant No. 2016YFC0206507). This work was supported by access to
557 equipment made possible by the Hope Center for Neurological Disorders and the Departments of
558 Neurology and Psychiatry at Washington University School of Medicine.

559

560 **Author Contributions**

561 A.M.G., E.M., and K.H. conceived and designed the experiments. K.H., S.C.J., O.H., A.D., M.K.,
562 J.C., J.C.L., V.C., C.B., B.G., Y.D., A.M., T.R., A.R., J.L.D., M.V.F, L.I., B.Z., I.B., C.C. and
563 E.M. performed data analysis. A.A.P. performed phagocytosis assays, western blotting and
564 qPCR validation. S.B., B.P.F., J.B., R.S., V.E.P., R.M., J.L.H., L.A.F., M.A.P., S.S., J.W., P.A.,
565 G.D.S., J.S.K.K., K.H., and C.C. provided and processed the data. A.M.G. supervised data
566 analysis and functional experiments. K.H., A.A.P., E.M., and A.M.G. wrote and edited the
567 manuscript. All authors read and approved the manuscript.

568

569 **Competing Financial Interests Statement**

570 I.B. is an employee of Regeneron Pharmaceuticals, Inc. A.M.G. is on the scientific advisory
571 board for Denali Therapeutics and has served as a consultant for AbbVie and Cognition
572 Therapeutics.

573

574

575 **Figure Legends**

576

577 **Figure 1. Genetic and eQTL fine-mapping of AD.** (a) The AD-survival association landscape
578 at the *CELF1/SPI1* locus resembles that of *SPI1* eQTL association in monocytes and
579 macrophages. (b) The AD-survival association landscape resembles that of *MS4A4A/MS4A6A*
580 eQTL association in monocytes and macrophages.

581

582 **Figure 2. *SPI1* (PU.1) expression and ChIP-Seq analysis.** (a) Rs1057233^G is associated with
583 reduced *SPI1* expression in a dosage-dependent manner. (b) The mouse homolog of *SPI1*, *Sfpil*
584 or *Spi1*, is selectively expressed in microglia and macrophages in mouse brains based on the
585 brain RNA-Seq database²⁹⁻³¹. OPCs contain 5% microglial contamination. (c) *SPI1* (PU.1) binds
586 to the promoter and regulatory regions of *CD33*, *MS4A4A*, *MS4A6A*, *TREM2*, and *TREML2* in
587 human CD14+ monocytes based on ChIP-Seq data³⁵.

588

589 **Figure 3. PU.1 modulates the phagocytic activity of BV2 microglial cells.** (a) Phagocytosis of
590 zymosan labeled with red pHrodo fluorescent dye in BV2 cells with transient overexpression and
591 knock-down of PU.1 was measured by flow cytometry. Cytochalasin D treatment was used as a
592 negative control. Mean phagocytic index \pm SD is shown: pcDNA 0.7373 \pm 0.1772, pcDNA + 1
593 μ M Cyt 0.0236 \pm 0.0242, FLAG-PU.1 1.2630 \pm 0.2503, shSCR 1.014 \pm 0.3656, shA 0.4854 \pm
594 0.1209, shB 0.2579 \pm 0.06967, shD 0.2002 \pm 0.05168. $F(6,13) = 14.82$, pcDNA vs pcDNA + 1
595 μ M Cyt $P=0.0078$, pcDNA vs FLAG-PU.1 $P=0.0295$, shSCR vs shA $P=0.0283$, shSCR vs shB
596 $P=0.0020$, shSCR vs shD $P=0.0010$, $n = 3$. (b) BV2 cells were transiently transfected with
597 pcDNA3 (pcDNA) or pcDNA3-FLAG-PU.1 (FLAG-PU.1) and pCMV-GFP as described for
598 phagocytosis assay. Note a shift in mobility of the band for exogenous FLAG-PU.1 in
599 overexpression condition compared to endogenous PU.1 in control. (c) BV2 cells were
600 transiently transfected with shRNA targeting PU.1 (shA, shB and shD) or non-targeting control
601 (shSCR) in pGFP-V-RS vector. GFP⁺ cells were sorted with flow cytometer and analyzed for
602 levels of PU.1 in western blotting in two independent experiments (b, c). (d) Quantification of
603 PU.1 levels in c normalized to β -Actin as a loading control. Values are presented as mean \pm SD:
604 shSCR 100 \pm 2.10, shA 50.34 \pm 9.52, shB 16.03 \pm 14.72, shD 12.13 \pm 10.03. $F(3,6) = 70.55$,
605 shSCR vs shA $P=0.0014$, shSCR vs shB $P < 0.0001$, shSCR vs shD $P < 0.0001$, $n = 2$. * $P < 0.05$,
606 ** $P < 0.01$, *** $P < 0.001$, one-way ANOVA with Sidak's post hoc multiple comparisons test
607 between selected groups.

608

609 **Figure 4. Genes regulated with differential expression of *Spi1* in BV2 microglial cells.** qPCR
610 analysis in transiently transfected and sorted GFP⁺ BV2 cells with overexpression (FLAG-PU.1)
611 and knock-down (shB) of *Spi1*. Changes in expression levels are grouped for genes with altered
612 levels after overexpression and knock-down of *Spi1* in (a) and genes with variable expression in
613 BV2 cells either with overexpression (b) or knock-down (c) of *Spi1*. Values are presented as
614 mean \pm SD, $n = 4$ samples collected independently. * $P < 0.05$, ** $P < 0.01$, *** $P < 0.001$, one-
615 way ANOVA with Dunnett's post hoc multiple comparisons test between experimental and
616 control groups, detailed statistical analysis is reported in **Supplementary Table 11**.

617

618

619

620 **Tables**

621 **Table 1. Genome-wide survival analysis of Alzheimer’s Disease.** (a) Description of Consortia
 622 samples with available phenotype and genotype data included in the genome-wide survival
 623 analysis. AAO: age at onset. AAE: age at last examination. (b) Summary of loci with significant
 624 ($P < 5 \times 10^{-8}$) or suggestive ($P < 1 \times 10^{-5}$) associations from the genome-wide survival analysis.

625 a

Dataset	Cases			Controls		
	N	Percent women	Mean AAO yrs (s.d.)	N	Percent women	Mean AAE yrs (s.d.)
ADGC	8617	58.9	74.2 (8.1)	9765	60.1	77.1 (8.4)
GERAD	2615	63.4	73.0 (8.5)	1148	62.1	76.5 (7.0)
EADI case-control study	1420	67.2	72.1 (7.1)	878	61	72.2 (7.8)
EADI longitudinal study	387	61.8	81.3 (5.6)	5416	61.1	79.3 (5.3)
CHARGE FHS	229	65.5	85.7 (6.3)	1979	54.1	80.7 (7.5)
CHARGE CHS	374	69.2	82.2 (5.0)	1675	60.6	81.1 (5.2)
CHARGE Rotterdam	764	73.2	83.1 (6.6)	4988	57.8	81.4 (6.9)
Total	14406	61.7	74.8	25849	59.6	79.0

626 b

SNP	Major/minor Alleles	MAF	CHR ^a	BP	Closest Gene	Logistic OR ^b	Logistic P value	Survival HR (95% CI) ^c	Survival P value	Heterogeneity P value
<i>Previously reported associated loci</i>										
rs2093761	G/A	0.2019	1	207786542	<i>CRI</i>	1.16 (1.12-1.20)	2.6x10 ⁻¹⁴	1.07 (1.04-1.10)	1.2x10 ⁻⁶	0.25
rs6431219	C/T	0.4163	2	127862133	<i>BINI</i>	1.12 (1.09-1.15)	7.6x10 ⁻¹³	1.08 (1.06-1.10)	3.9x10 ⁻¹⁰	0.16
rs1057233	A/G	0.3194	11	47376448	<i>SPI1/CELF1^d</i>	0.93 (0.89-0.96)	5.4x10 ⁻⁶	0.94 (0.91-.97)	8.4x10 ⁻⁶	0.86
rs7930318	T/C	0.4004	11	60033371	<i>MS4A</i>	0.90 (0.87-0.93)	5.1x10 ⁻¹¹	0.93 (0.90-.95)	2.3x10 ⁻⁹	0.6
rs567075	C/T	0.3097	11	85830157	<i>PICALM</i>	0.88 (0.85-0.91)	4.3x10 ⁻¹⁴	0.91 (0.89-.94)	9.1x10 ⁻¹²	0.74
rs9665907	G/A	0.1133	11	121435470	<i>SORL1</i>	0.88 (0.83-0.93)	1.8x10 ⁻⁷	0.92 (0.88-.95)	5.5x10 ⁻⁶	0.96
rs17125944	T/C	0.0924	14	53400629	<i>FERMT2</i>	1.13 (1.08-1.18)	1.0x10 ⁻⁵	1.10 (1.06-1.14)	2.3x10 ⁻⁶	0.31
rs4803758	G/T	0.3551	19	45327423	<i>APOE^e</i>	1.33 (1.30-1.37)	1.2x10 ⁻⁶⁷	1.21 (1.18-1.23)	7.8x10 ⁻⁵²	0.32
<i>Novel loci reaching suggestive significance</i>										
rs10919252	C/G	0.3275	1	169802956	<i>C1orf112</i>	1.04 (1.01-1.08)	1.1x10 ⁻²	1.10 (1.06-1.14)	8.2x10 ⁻⁷	0.92
rs1532244	A/G	0.0925	3	28057905	<i>CMC1</i>	0.95 (0.90-1.01)	6.9x10 ⁻²	0.86 (0.80-.93)	9.7x10 ⁻⁶	0.99
rs116341973	A/G	0.0227	3	63462893	<i>SYNPR</i>	1.20 (1.09-1.30)	5.4x10 ⁻⁴	1.23 (1.15-1.31)	2.5x10 ⁻⁷	0.62
rs71602496	A/G	0.1453	4	661002	<i>PDE6B</i>	1.02 (0.98-1.06)	3.6x10 ⁻¹	1.08 (1.05-1.11)	5.0x10 ⁻⁶	0.11
rs1689013	T/C	0.2493	4	181048651	<i>LINC00290</i>	1.02 (0.98-1.06)	2.7x10 ⁻¹	1.07 (1.04-1.09)	4.7x10 ⁻⁶	0.31
rs7445192	A/G	0.461	5	140138701	<i>PCDHAI</i>	NA	NA	1.06 (1.03-1.08)	7.9x10 ⁻⁶	0.77
rs12207208	T/C	0.1034	6	40301379	<i>LINC00951</i>	1.07 (1.02-1.20)	1.2x10 ⁻²	1.09 (1.05-1.13)	6.8x10 ⁻⁶	0.78
rs17170228	G/A	0.0623	7	33076314	<i>NT5C3A</i>	1.07 (1.01-1.14)	2.5x10 ⁻²	1.13 (1.08-1.18)	1.0x10 ⁻⁶	0.94
rs2725066	A/T	0.4872	8	4438058	<i>CSMD1</i>	1.03 (1.00-1.06)	7.3x10 ⁻²	1.10 (1.06-1.14)	1.0x10 ⁻⁶	0.6
rs7867518	T/C	0.476	9	2527525	<i>VLDLR</i>	0.97 (0.94-1.00)	6.8x10 ⁻²	0.95 (0.92-.97)	9.1x10 ⁻⁶	0.79

rs1625716	T/G	0.0643	10	59960083	<i>IPMK</i>	0.87 (0.80-0.94)	1.0x10 ⁻⁴	0.88 (0.82-.94)	7.7x10 ⁻⁶	0.95
rs1118069	T/A	0.2805	12	84739181	<i>SLC6A15</i>	0.98 (0.94-1.01)	2.0x10 ⁻¹	0.90 (0.86-.95)	2.7x10 ⁻⁶	0.8
rs11074412	A/G	0.2087	16	19833001	<i>IQCK</i>	0.94 (0.90-0.98)	1.9x10 ⁻³	0.93 (0.90-.96)	7.0x10 ⁻⁶	0.48
rs5750677	C/T	0.2885	22	39147715	<i>SUN2</i>	0.97 (0.93-1.00)	5.1x10 ⁻²	0.94 (0.91-.97)	5.2x10 ⁻⁶	0.51

aBuild 37, assembly hg19. ^bSummary statistics of the logistic regression were obtained from stage 1 of the IGAP GWAS. ^cCalculated with respect to the minor allele. ^d*SPII* is the nearest gene to rs1057233. The same locus was previously labeled as *CELF1* in the 2013 IGAP GWAS paper¹. ^eThe nearest gene to rs4803758 is *APOE*.

627
628
629
630
631

632 **Table 2. Summary of CSF biomarker-associations of suggestive and significant AAOS-**
 633 **associated SNPs.** Associations reaching the significance threshold after Bonferroni correction
 634 for multiple testing ($P < 2.27 \times 10^{-3}$) are bolded.

SNP	CHR	Closest gene	Beta _{tau}	P _{tau}	Beta _{ptau}	P _{ptau}	Beta _{ab42}	P _{ab42}
<i>Previously reported associated loci</i>								
rs2093761	1	<i>CRI</i>	-	>0.05	1.46x10 ⁻²	2.87x10 ⁻²	-	>0.05
rs6431219	2	<i>BINI</i>	-	>0.05	-	>0.05	-	>0.05
rs1057233	11	<i>CELF1</i>	-1.11x10 ⁻²	6.55x10 ⁻²	-1.25x10 ⁻²	2.76x10 ⁻²	1.45x10⁻²	8.24x10⁻⁴
rs7930318	11	<i>MS4A</i>	-1.24x10 ⁻²	3.27x10 ⁻²	-	>0.05	-	>0.05
rs567075	11	<i>PICALM</i>	-1.32x10 ⁻²	3.22x10 ⁻²	-1.24x10 ⁻²	3.13x10 ⁻²	9.10x10 ⁻³	3.88x10 ⁻²
rs9665907	11	<i>SORL1</i>	-1.74x10 ⁻²	4.28x10 ⁻²	-1.94x10 ⁻²	1.57x10 ⁻²	-	>0.05
rs17125944	14	<i>FERMT2</i>	2.50x10 ⁻²	8.71x10 ⁻³	2.09x10 ⁻²	2.09x10 ⁻²	-1.79x10 ⁻²	8.90x10 ⁻³
rs4803758	19	<i>APOE</i>	1.61x10 ⁻²	7.42x10 ⁻³	2.01x10⁻²	3.75x10⁻⁴	-1.79x10⁻²	3.12x10⁻⁵
<i>Novel candidate loci</i>								
rs10919252	1	<i>C1orf112</i>	-	>0.05	-	>0.05	-	>0.05
rs1532244	3	<i>CMC1</i>	-	>0.05	2.41x10 ⁻²	1.23x10 ⁻²	-	>0.05
rs116341973	3	<i>SYNPR</i>	-	>0.05	-	>0.05	-	>0.05
rs71602496	4	<i>PDE6B</i>	-	>0.05	-	>0.05	-	>0.05
rs1689013	4	<i>LINC00290</i>	-	>0.05	-	>0.05	-	>0.05
rs7445192	5	<i>PCDHA1</i>	-	>0.05	1.38x10 ⁻²	9.98x10 ⁻³	-	>0.05
rs12207208	6	<i>LINC00951</i>	-	>0.05	-	>0.05	-	>0.05
rs17170228	7	<i>NT5C3A</i>	-	>0.05	-	>0.05	-	>0.05
rs2725066	8	<i>CSMD1</i>	1.20x10 ⁻²	4.53x10 ⁻²	-	>0.05	-	>0.05
rs7867518	9	<i>VLDLR</i>	-1.58x10 ⁻²	5.83x10 ⁻³	-	>0.05	-	>0.05
rs1625716	10	<i>IPMK</i>	-	>0.05	-	>0.05	-	>0.05
rs1118069	12	<i>SLC6A15</i>	-	>0.05	-	>0.05	-1.07x10 ⁻²	1.56x10 ⁻²
rs11074412	16	<i>IQCK</i>	-	>0.05	-	>0.05	-	>0.05
rs5750677	22	<i>SUN2</i>	1.30x10 ⁻²	3.55x10 ⁻²	-	>0.05	-	>0.05

635
636

637 **Table 3. Significant *cis*-eQTL associations of the 22 suggestive and significant AAOS-**
 638 **associated SNPs.** Significance threshold is determined to be 2.52×10^{-6} based on Bonferroni
 639 correction for multiple testing. The minor alleles are considered as the effective allele.

SNPID	CHR	Probe Id	Gene	Monocyte		Macrophage	
				P value	Beta	P value	Beta
rs10919252	1	ILMN_1724422	<i>SELL</i>	7.33×10^{-35}	-0.65	-	-
rs71602496	4	ILMN_1769751	<i>PIGG</i>	5.19×10^{-10}	-0.46	9.11×10^{-13}	-0.58
rs1625716	10	ILMN_2122953	<i>CISD1</i>	5.98×10^{-23}	-1.09	7.82×10^{-8}	-0.67
rs1057233	11	ILMN_1696463	<i>SPII</i>	1.50×10^{-105}	-1.11	6.41×10^{-87}	-1.11
rs1057233	11	ILMN_1781184	<i>MYBPC3</i>	4.99×10^{-51}	-0.83	5.58×10^{-23}	-0.62
rs1057233	11	ILMN_1686516	<i>CELF1</i>	3.95×10^{-8}	0.32	-	-
rs1057233	11	ILMN_2382083	<i>CELF1</i>	1.13×10^{-7}	0.31	1.31×10^{-4}	0.25
rs1057233	11	ILMN_1652989	<i>NUP160</i>	1.42×10^{-5}	-0.26	5.35×10^{-22}	-0.62
rs7930318	11	ILMN_2370336	<i>MS4A4A</i>	8.20×10^{-28}	-0.56	-	-
rs7930318	11	ILMN_1721035	<i>MS4A6A</i>	4.90×10^{-23}	-0.52	1.25×10^{-9}	-0.35
rs7930318	11	ILMN_1741712	<i>MS4A4A</i>	1.48×10^{-11}	-0.36	1.54×10^{-4}	-0.22
rs7930318	11	ILMN_2359800	<i>MS4A6A</i>	1.94×10^{-10}	-0.34	3.77×10^{-9}	-0.34
rs11074412	16	ILMN_1783712	<i>LOC400506</i>	6.49×10^{-17}	0.54	-	-
rs11074412	16	ILMN_2081883	<i>IQCK</i>	-	-	1.22×10^{-12}	-0.52
rs4803758	19	ILMN_2337336	<i>PVRL2</i>	1.52×10^{-8}	0.30	-	-
rs5750677	22	ILMN_2099301	<i>SUN2</i>	3.66×10^{-58}	-0.90	3.15×10^{-36}	-0.80
rs5750677	22	ILMN_1730879	<i>CBY1</i>	1.80×10^{-9}	-0.37	-	-

640
641

642 **Reference**

- 643 1. Lambert, J.-C. *et al.* Meta-analysis of 74,046 individuals identifies 11 new susceptibility
644 loci for Alzheimer's disease. *Nat. Genet.* **45**, 1452–8 (2013).
- 645 2. Naj, A. C. *et al.* Common variants at MS4A4/MS4A6E, CD2AP, CD33 and EPHA1 are
646 associated with late-onset Alzheimer's disease. *Nat Genet* **43**, 436–441 (2011).
- 647 3. Harold, D. *et al.* Genome-wide association study identifies variants at CLU and PICALM
648 associated with Alzheimer's disease. *Nat Genet* **41**, 1088–1093 (2009).
- 649 4. Seshadri, S. *et al.* Genome-wide analysis of genetic loci associated with Alzheimer
650 disease. *JAMA* **303**, 1832–40 (2010).
- 651 5. Hollingworth, P. *et al.* Common variants at ABCA7, MS4A6A/MS4A4E, EPHA1, CD33
652 and CD2AP are associated with Alzheimer's disease. *Nat Genet* **43**, 429–435 (2011).
- 653 6. Naj, A. C. *et al.* Effects of Multiple Genetic Loci on Age at Onset in Late-Onset
654 Alzheimer Disease: A Genome-Wide Association Study. *JAMA Neurol* (2014).
655 doi:10.1001/jamaneurol.2014.1491
- 656 7. Kamboh, M. I. *et al.* Genome-wide association analysis of age-at-onset in Alzheimer's
657 disease. *Mol. Psychiatry* **17**, 1340–6 (2012).
- 658 8. Bennett, C. *et al.* Evidence that the APOE locus influences rate of disease progression in
659 late onset familial Alzheimer's Disease but is not causative. *Am J Med Genet* **60**, 1–6
660 (1995).
- 661 9. Slooter, A. J. *et al.* Risk estimates of dementia by apolipoprotein E genotypes from a
662 population-based incidence study: the Rotterdam Study. *Arch Neurol* **55**, 964–968 (1998).
- 663 10. Thambisetty, M., An, Y. & Tanaka, T. Alzheimer's disease risk genes and the age-at-onset
664 phenotype. *Neurobiol Aging* **34**, 2696 e1-5 (2013).
- 665 11. Jones, E. L. *et al.* Evidence that PICALM affects age at onset of Alzheimer's dementia in
666 Down syndrome. *Neurobiol Aging* **34**, 2441 e1-5 (2013).
- 667 12. Cruchaga, C. *et al.* GWAS of cerebrospinal fluid tau levels identifies risk variants for
668 alzheimer's disease. *Neuron* **78**, 256–268 (2013).
- 669 13. Kauwe, J. S. K. *et al.* Alzheimer's disease risk variants show association with
670 cerebrospinal fluid amyloid beta. *Neurogenetics* **10**, 13–17 (2009).
- 671 14. Gusev, A. *et al.* Integrative approaches for large-scale transcriptome-wide association
672 studies. *Nat. Genet.* **48**, 245–52 (2016).
- 673 15. Jonsson, T. *et al.* Variant of TREM2 associated with the risk of Alzheimer's disease. *N*
674 *Engl J Med* **368**, 107–116 (2013).
- 675 16. Guerreiro, R. *et al.* TREM2 variants in Alzheimer's disease. *N Engl J Med* **368**, 117–127
676 (2013).
- 677 17. Bradshaw, E. M. *et al.* CD33 Alzheimer's disease locus: altered monocyte function and
678 amyloid biology. *Nat. Neurosci.* **16**, 848–50 (2013).
- 679 18. Zhang, B. *et al.* Integrated systems approach identifies genetic nodes and networks in late-
680 onset Alzheimer's disease. *Cell* **153**, 707–20 (2013).
- 681 19. Gjoneska, E. *et al.* Conserved epigenomic signals in mice and humans reveal immune
682 basis of Alzheimer's disease. *Nature* **518**, 365–369 (2015).
- 683 20. Chan, G. *et al.* CD33 modulates TREM2: convergence of Alzheimer loci. *Nat. Neurosci.*
684 (2015). doi:10.1038/nn.4126
- 685 21. Raj, T. *et al.* Polarization of the effects of autoimmune and neurodegenerative risk alleles
686 in leukocytes. *Science* **344**, 519–23 (2014).
- 687 22. Kamboh, M. I. *et al.* Genome-wide association analysis of age-at-onset in Alzheimer's

- 688 disease. *Mol Psychiatry* **17**, 1340–1346 (2012).
- 689 23. Zhu, Z. *et al.* Integration of summary data from GWAS and eQTL studies predicts
690 complex trait gene targets. *Nat. Genet.* **48**, 481–7 (2016).
- 691 24. GTEx Consortium, T. Gte. The Genotype-Tissue Expression (GTEx) project. *Nat. Genet.*
692 **45**, 580–5 (2013).
- 693 25. Finucane, H. K. *et al.* Partitioning heritability by functional annotation using genome-
694 wide association summary statistics. *Nat. Genet.* **47**, 1228–1235 (2015).
- 695 26. Cross-Disorder Group of the Psychiatric Genomics Consortium. Identification of risk loci
696 with shared effects on five major psychiatric disorders: a genome-wide analysis. *Lancet*
697 **381**, 1371–9 (2013).
- 698 27. Garnier, S. *et al.* Genome-Wide Haplotype Analysis of Cis Expression Quantitative Trait
699 Loci in Monocytes. *PLoS Genet.* **9**, (2013).
- 700 28. Fairfax, B. P. *et al.* Innate immune activity conditions the effect of regulatory variants
701 upon monocyte gene expression. *Science* **343**, 1246949 (2014).
- 702 29. Zhang, Y. *et al.* Purification and Characterization of Progenitor and Mature Human
703 Astrocytes Reveals Transcriptional and Functional Differences with Mouse. *Neuron* **89**,
704 37–53 (2016).
- 705 30. Zhang, Y. *et al.* An RNA-Sequencing Transcriptome and Splicing Database of Glia,
706 Neurons, and Vascular Cells of the Cerebral Cortex. *J. Neurosci.* **34**, 11929–47 (2014).
- 707 31. Bennett, M. L. *et al.* New tools for studying microglia in the mouse and human CNS. *Proc.*
708 *Natl. Acad. Sci. U. S. A.* **113**, E1738-1746 (2016).
- 709 32. Giambartolomei, C. *et al.* Bayesian Test for Colocalisation between Pairs of Genetic
710 Association Studies Using Summary Statistics. *PLoS Genet.* **10**, (2014).
- 711 33. Hikami, K. *et al.* Association of a functional polymorphism in the 3'-untranslated region
712 of SPI1 with systemic lupus erythematosus. *Arthritis Rheum.* **63**, 755–63 (2011).
- 713 34. Ward, L. D. & Kellis, M. HaploReg: A resource for exploring chromatin states,
714 conservation, and regulatory motif alterations within sets of genetically linked variants.
715 *Nucleic Acids Res.* **40**, (2012).
- 716 35. Pham, T. H. *et al.* Dynamic epigenetic enhancer signatures reveal key transcription factors
717 associated with monocytic differentiation states. *Blood* **119**, (2012).
- 718 36. Steinberg, S. *et al.* Loss-of-function variants in ABCA7 confer risk of Alzheimer's disease.
719 *Nat. Genet.* **47**, 445–7 (2015).
- 720 37. Bernstein, B. E. *et al.* An integrated encyclopedia of DNA elements in the human genome.
721 *Nature* **489**, 57–74 (2012).
- 722 38. Sakai, K. *et al.* A neuronal VLDLR variant lacking the third complement-type repeat
723 exhibits high capacity binding of apoE containing lipoproteins. *Brain Res.* **1276**, 11–21
724 (2009).
- 725 39. Bajari, T. M., Strasser, V., Nimpf, J. & Schneider, W. J. A model for modulation of leptin
726 activity by association with clusterin. *FASEB J.* **17**, 1505–7 (2003).
- 727 40. Speliotes, E. K. *et al.* Association analyses of 249,796 individuals reveal 18 new loci
728 associated with body mass index. *Nat. Genet.* **42**, 937–48 (2010).
- 729 41. Strawbridge, R. J. *et al.* Genome-wide association identifies nine common variants
730 associated with fasting proinsulin levels and provides new insights into the
731 pathophysiology of type 2 diabetes. *Diabetes* **60**, 2624–34 (2011).
- 732 42. Satoh, J.-I., Asahina, N., Kitano, S. & Kino, Y. A Comprehensive Profile of ChIP-Seq-
733 Based PU.1/Spi1 Target Genes in Microglia. *Gene Regul. Syst. Bio.* **8**, 127–39 (2014).

- 734 43. Daniel, B. *et al.* The active enhancer network operated by liganded RXR supports
735 angiogenic activity in macrophages. *Genes Dev.* **28**, 1562–1577 (2014).
- 736 44. McKercher, S. R. *et al.* Targeted disruption of the PU.1 gene results in multiple
737 hematopoietic abnormalities. *EMBO J.* **15**, 5647–58 (1996).
- 738 45. Beers, D. R. *et al.* Wild-type microglia extend survival in PU.1 knockout mice with
739 familial amyotrophic lateral sclerosis. *Proc. Natl. Acad. Sci. U. S. A.* **103**, 16021–6 (2006).
- 740 46. Mak, K. S., Funnell, A. P. W., Pearson, R. C. M. & Crossley, M. PU.1 and haematopoietic
741 cell fate: Dosage matters. *International Journal of Cell Biology* (2011).
742 doi:10.1155/2011/808524
- 743 47. Smith, A. M. *et al.* The transcription factor PU.1 is critical for viability and function of
744 human brain microglia. *Glia* **61**, 929–942 (2013).
- 745 48. Butovsky, O. *et al.* Identification of a unique TGF- β -dependent molecular and functional
746 signature in microglia. *Nat. Neurosci.* **17**, 131–43 (2014).
- 747 49. Wang, Y. *et al.* IL-34 is a tissue-restricted ligand of CSF1R required for the development
748 of Langerhans cells and microglia. *Nat. Immunol.* **13**, 753–60 (2012).
- 749 50. Dagher, N. N. *et al.* Colony-stimulating factor 1 receptor inhibition prevents microglial
750 plaque association and improves cognition in 3xTg-AD mice. *J. Neuroinflammation* **12**,
751 139 (2015).
752
753
754
755
756
757

758 **Online Methods**

759 *Genome-wide survival association study datasets*

760 The final meta-analysis dataset consists of samples from the Alzheimer's Disease Genetics
761 Consortium (ADGC), Genetic and Environmental Risk in Alzheimer's Disease (GERAD),
762 European Alzheimer's Disease Initiative (EADI), and Cohorts for Heart and Aging Research in
763 Genomic Epidemiology (CHARGE). The study cohorts consist of case-control and longitudinal
764 cohorts. For all studies, written informed consent was obtained from study participants or, for
765 those with substantial cognitive impairment, from a caregiver, legal guardian, or other proxy, and
766 the study protocols for all populations were reviewed and approved by the appropriate
767 Institutional review boards. Details of ascertainment and diagnostic procedures for each dataset
768 extend from details previously described¹⁻⁵ and are documented below:

770 (1) Alzheimer's Disease Genetics Consortium (ADGC)

771 The imputed ADGC sample that passed quality control procedures comprised of 8,617 AD cases
772 and 9,765 control subjects from GWAS datasets assembled by the Alzheimer's Disease Genetics
773 Consortium (ADGC). Details of ascertainment and diagnostic procedures for each data set were
774 as previously described².

776 (2) Genetic and Environmental Risk in Alzheimer's Disease (GERAD)

777 Data used in the preparation of this article were obtained from the Genetic and Environmental
778 Risk for Alzheimer's disease (GERAD) Consortium. The imputed GERAD sample comprised
779 3,177 AD cases and 7,277 controls with available age and gender data. A subset of this sample
780 has been used in this study, comprising 2,615 cases and 1,148 elderly screened controls. Cases
781 and elderly screened controls were recruited by the Medical Research Council (MRC) Genetic
782 Resource for AD (Cardiff University; Institute of Psychiatry, London; Cambridge University;
783 Trinity College Dublin), the Alzheimer's Research UK (ARUK) Collaboration (University of
784 Nottingham; University of Manchester; University of Southampton; University of Bristol;
785 Queen's University Belfast; the Oxford Project to Investigate Memory and Ageing (OPTIMA),
786 Oxford University); Washington University, St Louis, United States; MRC PRION Unit,
787 University College London; London and the South East Region AD project (LASER-AD),
788 University College London; Competence Network of Dementia (CND) and Department of
789 Psychiatry, University of Bonn, Germany; the National Institute of Mental Health (NIMH)AD
790 Genetics Initiative. 6,129 population controls were drawn from large existing cohorts with
791 available GWAS data, including the 1958 British Birth Cohort (1958BC)
792 (<http://www.b58cgene.sgul.ac.uk>), the KORA F4 Study and the Heinz Nixdorf Recall Study. All
793 AD cases met criteria for either probable (NINCDS-ADRDA, DSM-IV) or definite (CERAD)
794 AD. All elderly controls were screened for dementia using the MMSE or ADAS-cog, were
795 determined to be free from dementia at neuropathological examination or had a Braak score of
796 2.5 or lower. Genotypes from all cases and 4,617 controls were previously included in the AD
797 GWAS by Harold and colleagues (2009). Genotypes for the remaining 2,660 population controls
798 were obtained from WTCCC2. Imputation of the dataset was performed using IMPUTE2 and the
799 1000 genomes (<http://www.1000genomes.org/>) Dec2010 reference panel (NCBI build 37.1). The
800 imputed data was then analysed using logistic regression including covariates for country of
801 origin, gender, age and 3 principal components obtained with EIGENSTRAT software based on
802 individual genotypes for the GERAD study participants.

803 GERAD Supplementary Acknowledgements: This study incorporated imputed summary results
804 from the GERAD1 genome-wide association study. GERAD Acknowledgements: Cardiff
805 University was supported by the Wellcome Trust, Medical Research Council (MRC),
806 Alzheimer's Research UK (ARUK) and the Welsh Assembly Government. Cambridge
807 University and Kings College London acknowledge support from the MRC. ARUK supported
808 sample collections at the South West Dementia Bank and the Universities of Nottingham,
809 Manchester and Belfast. The Belfast group acknowledges support from the Alzheimer's Society,
810 Ulster Garden Villages, N.Ireland R&D Office and the Royal College of Physicians/Dunhill
811 Medical Trust. The MRC and Mercer's Institute for Research on Ageing supported the Trinity
812 College group. The South West Dementia Brain Bank acknowledges support from Bristol
813 Research into Alzheimer's and Care of the Elderly. The Charles Wolfson Charitable Trust
814 supported the OPTIMA group. Washington University was funded by NIH grants, Barnes Jewish
815 Foundation and the Charles and Joanne Knight Alzheimer's Research Initiative. Patient
816 recruitment for the MRC Prion Unit/UCL Department of Neurodegenerative Disease collection
817 was supported by the UCLH/UCL Biomedical Centre and NIHR Queen Square Dementia
818 Biomedical Research Unit. LASER-AD was funded by Lundbeck SA. The Bonn group was
819 supported by the German Federal Ministry of Education and Research (BMBF), Competence
820 Network Dementia and Competence Network Degenerative Dementia, and by the Alfred Krupp
821 von Bohlen und Halbach-Stiftung. The GERAD Consortium also used samples ascertained by
822 the NIMH AD Genetics Initiative.

823 The KORA F4 studies were financed by Helmholtz Zentrum München; German Research Center
824 for Environmental Health; BMBF; German National Genome Research Network and the Munich
825 Center of Health Sciences. The Heinz Nixdorf Recall cohort was funded by the Heinz Nixdorf
826 Foundation (Dr. jur. G.Schmidt, Chairman) and BMBF. Coriell Cell Repositories is supported by
827 NINDS and the Intramural Research Program of the National Institute on Aging. We
828 acknowledge use of genotype data from the 1958 Birth Cohort collection, funded by the MRC
829 and the Wellcome Trust which was genotyped by the Wellcome Trust Case Control Consortium
830 and the Type-1 Diabetes Genetics Consortium, sponsored by the National Institute of Diabetes
831 and Digestive and Kidney Diseases, National Institute of Allergy and Infectious Diseases,
832 National Human Genome Research Institute, National Institute of Child Health and Human
833 Development and Juvenile Diabetes Research Foundation International.

834

835 (3) European Alzheimer's Disease Initiative (EADI)

836 All AD cases were ascertained by neurologists from Bordeaux, Dijon, Lille, Montpellier, Paris,
837 and Rouen, with clinical diagnosis of probable AD established according to the DSM-III-R and
838 National Institute of Neurological and Communication Disorders and Stroke-Alzheimer's
839 Disease and Related Disorders Association (NINCDS-ADRDA) criteria^{51,52}. Controls were
840 recruited from Lille, Rouen, Nantes and from the 3C Study⁵¹. This cohort is a population-based,
841 prospective study of the relationship between vascular factors and dementia. It has been carried
842 out in three French cities: Bordeaux (southwest France), Montpellier (southeast France) and
843 Dijon (central eastern France). A sample of non-institutionalized, subjects over 65 years was
844 randomly selected from the electoral rolls of each city. Between January 1999 and March 2001,
845 9,686 subjects meeting the inclusion criteria agreed to participate. Following recruitment, 392
846 subjects withdrew from the study. Thus, 9,294 subjects were finally included in the study (2,104
847 in Bordeaux, 4,931 in Dijon and 2,259 in Montpellier). At 8 years of follow up, 664 individuals
848 suffered from AD with 167 prevalent and 497 incident cases. The other individuals were

849 considered as controls. 9863 DNA samples that passed DNA quality control were genotyped
850 with Illumina Human 610-Quad BeadChips. Following quality control procedures, a final sample
851 size of 5,803 3C individuals (387 AD cases and 5,416 controls, cohort dataset) and 2,298 non-3C
852 individuals (1,420 AD cases and 878 controls, case-control dataset) was included in this study.

853
854 (4) Cohorts for Heart and Aging Research in Genomic Epidemiology (CHARGE)
855 Cardiovascular Health Study (CHS): The CHS is a prospective population-based cohort study of
856 risk factors for vascular and metabolic disease that in 1989-90, enrolled adults aged ≥ 65 years, at
857 four field centers located in North Carolina, California, Maryland and Pennsylvania. The original
858 predominantly Caucasian cohort of 5,201 persons was recruited from a random sample of people
859 on Medicare eligibility lists and an additional 687 African-Americans were enrolled
860 subsequently for a total sample of 5,882. DNA was extracted from blood samples drawn on all
861 persons who consented to genetic testing at their baseline examination in 1989-90. In 2007-2008,
862 genotyping was performed at the General Clinical Research Center's Phenotyping/Genotyping
863 Laboratory at Cedars-Sinai using the Illumina 370CNV Duo \otimes BeadChip system on 3,980 CHS
864 participants who were free of cardiovascular disease (CVD) at baseline. The 1,908 persons
865 excluded for prevalent CVD had prevalent coronary heart disease (n=1,195), congestive heart
866 failure (n=86), peripheral vascular disease (n=93), valvular heart disease (n=20), stroke (n=166)
867 or transient ischemic attack (n=56). Some persons had more than one reason to be excluded and
868 for these individuals only the initial exclusionary event is listed. Because the other cohorts were
869 predominantly white, the African American CHS participants were excluded from this analysis
870 to limit errors secondary to population stratification. Among white participants genotyping was
871 attempted in 3,397 participants and was successful in 3295 persons. After excluding persons that
872 had either died prior to the start of the CHS cognition study in 1992 (see section 3 for details),
873 could not be evaluated completely for baseline cognitive status, and persons that had dementia
874 other than AD, a sample of 2,049 persons was available. The CHS study protocols were
875 approved by the Institutional review boards at the individual participating centers.
876 The AD sample for this study included all prevalent cases identified in 1992 and incident events
877 identified between 1992 and December 20063. Briefly, persons were examined annually from
878 enrollment to 1999. The examination included a 30 minute screening cognitive battery. In 1992-
879 94 and again, in 1997-99, participants were invited to undergo brain MRI and detailed cognitive
880 and neurological assessment as part of the CHS Cognition Study. Persons with prevalent
881 dementia were identified, and all others were followed until 1999 for the development of
882 incident dementia and AD. Since then, CHS participants at the Maryland and Pennsylvania
883 centers have remained under ongoing dementia surveillance⁵³.
884 Beginning in 1988/89, all participants completed the Modified Mini-Mental State Examination
885 (3MSE) and the DSST at their annual visits, and the Benton Visual Retention Test (BVRT) from
886 1994 to 1998. The Telephone Interview for Cognitive Status (TICS) was used when participants
887 did not come to the clinic. Further information on cognition was obtained from proxies using the
888 Informant Questionnaire for Cognitive Decline in the Elderly (IQCODE), and the dementia
889 questionnaire (DQ). Symptoms of depression were measured with the modified version of the
890 Center for Epidemiology Studies Depression Scale (CES-D). In 1991-94, 3,608 participants had
891 an MRI of the brain and this was repeated in 1997-98. The CHS staff also obtained information
892 from participants and next-of-kin regarding vision and hearing, the circumstances of the illness,
893 history of dementia, functional status, pharmaceutical drug use, and alcohol consumption. Data

894 on instrumental activities of daily living (IADL), and activities of daily living (ADL) were also
895 collected.

896 Persons suspected to have cognitive impairment based on the screening tests listed above
897 underwent a neuropsychological and a neurological evaluation. The neuropsychological battery
898 included the following tests: the American version of the National Reading test (AMNART),
899 Raven's Coloured Progressive Matrices, California Verbal Learning Test (CVLT), a modified
900 Rey-Osterreith figure, the Boston Naming test, the Verbal fluency test, the Block design test, the
901 Trails A and B tests, the Baddeley & Papagno Divided Attention Task, the Stroop, Digit Span
902 and Grooved Pegboard Tests. The results of the neuropsychological battery were classified as
903 normal or abnormal (>1.5 standard deviations below individuals of comparable age and
904 education) based on normative data collected from a sample of 250 unimpaired subjects. The
905 neurological exam included a brief mental status examination, as well as a complete examination
906 of other systems. The examiner also completed the Unified Parkinson's Disease Rating Scale
907 (UPDRS) and the Hachinski Ischemic Scale. After completing the neurological exam, the
908 neurologist classified the participant as normal, having mild cognitive impairment (MCI), or
909 dementia.

910 International diagnostic guidelines, including the NINCDS-ADRDA criteria for probable and
911 possible AD and the ADDTC's State of California criteria for probable and possible vascular
912 dementia (VaD) with or without AD, were followed. CHS identified 3 subtypes:
913 possible/probable AD without VaD (categorized as pure AD, included in all AD) and mixed AD
914 (for cases that met criteria for both AD and VaD, included in all-AD), and, possible/probable
915 VaD without AD (excluded from current study).

916
917 Framingham Heart Study (FHS): The FHS is a three-generation, single-site, community-based,
918 ongoing cohort study that was initiated in 1948. It now comprises three generations of
919 participants including the Original cohort followed since 1948 ($n=5,209$)⁵⁴, their Offspring and
920 spouses of the offspring ($n=5,216$) followed since 1971⁵⁵; and children from the largest
921 Offspring families enrolled in 2000 (Gen 3)⁵⁶. Participants in the Original and Offspring cohorts
922 are used in these analyses, but Gen 3 participants were not included since they are young (mean
923 age 40 ± 9 years in 2000) and none had developed Alzheimer's Disease (AD). The Original cohort
924 enrolled 5,209 men and women who comprised two-thirds of the adult population then residing
925 in Framingham, Massachusetts. Survivors continue to receive biennial examinations. The
926 Offspring cohort comprises 5,124 persons (including 3,514 biological offspring) who have been
927 examined approximately once every 4 years. Almost all the FHS Original and Offspring
928 participants are white/Caucasian. FHS participants had DNA extracted and provided consent for
929 genotyping in the 1990s. All available eligible participants were genotyped at Affymetrix (Santa
930 Clara, CA) through an NHLBI funded SNP-Health Association Resource (SHARe) project using
931 the Affymetrix GeneChip® Human Mapping 500K Array Set and 50K Human Gene Focused
932 Panel®. In 272 persons, small amounts of DNA were extracted from stored whole blood and
933 required whole genome amplification prior to genotyping. Cell lines were available for most of
934 the remaining participants. Genotyping was attempted in 5,293 Original and Offspring cohort
935 participants, and 4,425 persons met QC criteria. Failures (call rate $<97\%$, extreme heterozygosity
936 or high Mendelian error rate) were largely restricted to persons with whole-genome amplified
937 DNA and DNA extracted from stored serum samples. In addition, since the persons with whole
938 genome amplified DNA represent a group of survivors who may differ from the others we
939 included whole genome amplified status as a covariate in FHS analyses. After exclusion of

940 prevalent dementia, dementia other than AD, and missing values, a sample of 2,208 participants
941 was available for this project. The FHS component of this study was approved by the
942 Institutional Review Board of the Boston Medical Center.
943 The Original cohort of the FHS has been evaluated biennially since 1948, was screened for
944 prevalent dementia and AD in 1974-76 and has been under surveillance for incident dementia
945 and AD since then⁵⁷⁻⁵⁹. The Offspring have been examined once every 4 years and have been
946 screened for prevalent dementia with a neuropsychological battery and brain MRI^{60,61}. In order to
947 be consistent with the sampling frame for the AGES and CHS samples, we excluded FHS
948 subjects with a baseline age <65 yrs at the time of DNA draw which was in the 1990s. To
949 minimize survival biases, Original cohort and Offspring participants who developed dementia
950 prior to the date of DNA draw were treated as prevalent cases, and subsequent events in the
951 Original cohort occurring prior to December 2006 were included in the incident analyses.
952 At each clinic exam, participants receive questionnaires, physical examinations and laboratory
953 testing; between examinations they remain under surveillance (regardless of whether or not they
954 live in the vicinity) via physician referrals, record linkage and annual telephone health history
955 updates. Methods used for dementia screening and follow-up have been previously described^{57,62}.
956 Briefly, surviving cohort members who attended biennial examination cycles 14 and 15 (May
957 1975-November 1979) were administered a standardized neuropsychological test battery to
958 establish a dementia-free cohort. Beginning at examination cycle 17 (1982), the MMSE was
959 administered biennially to the cohort. A MMSE score below the education-specific cutoff score,
960 a decline of 3 or more points on subsequent administrations, a decline of more than 5 points
961 compared with any previous examination, or a physician or family referral prompted further in-
962 depth testing. The Offspring cohort that was enrolled in 1971 has undergone 8 re-examinations,
963 one approximately every 4 years. Starting at the 2nd Offspring examination, participants were
964 questioned regarding any subjective memory complaints and since the 5th Offspring examination
965 participants have been administered the MMSE at each visit. In addition concurrent with the 7th
966 and 8th Offspring examinations (between 1999 and 2004 and then again between 2005 and 2009)
967 surviving Original cohort and all eligible and consenting Offspring participants have undergone
968 volumetric brain MRI and neuropsychological testing^{60,61}. The neuropsychological test battery
969 included the Reading subtest of the Wide Range Achievement Test (WRAT-3), the Logical
970 Memory and the Paired Associates Learning tests from the Wechsler Memory Scale, the Visual
971 Reproduction and Hooper Visual Organization Tests, Trails A and B, the Similarities subtest
972 from the Wechsler Adult Intelligence test, the 30-item version of the Boston Naming Test and at
973 the second assessment only, the Digit Span, Controlled Word Association and Clock Drawing
974 Tests. Offspring participants suspected to have cognitive impairment based on their MMSE
975 scores, participant, family or physician referral, hospital records or performance in the
976 neuropsychological test battery described above were referred for more detailed
977 neuropsychological and neurological evaluation.
978 Each participant thus identified underwent baseline neurologic and neuropsychological
979 examinations. Neurologists (trained in geriatric behavioral assessment) supplemented their
980 clinical assessment with a few structured cognitive tests and administered the Clinical Dementia
981 Rating (CDR). Persons were reassessed systematically for the onset of at least mild dementia. A
982 panel consisting of at least 1 neurologist (S.A., P.A.W., or S.S.) and 1 neuropsychologist (R.A.)
983 reviewed all available medical records to arrive at a final determination regarding the presence or
984 absence of dementia, the date of onset of dementia, and the type of dementia. For this
985 determination, we used data from the neurologist's examination, neuropsychological test

986 performance, Framingham Study records, hospital records, information from primary care
987 physicians, structured family interviews, computed tomography and magnetic resonance imaging
988 records, and autopsy confirmation when available. All individuals identified as having dementia
989 satisfied the DSM-IV criteria, had dementia severity equivalent to a CDR of 1 or greater, and had
990 symptoms of dementia for at least 6 months. All individuals identified as having Alzheimer-
991 related dementia met the NINCDS-ADRDA criteria for definite, probable, or possible AD.
992 Vascular Dementia was diagnosed using the ADDTC criteria but the presence of vascular
993 dementia did not disqualify a participant from obtaining a concomitant diagnosis of AD if
994 indicated. The recruitment of Original cohort participants at FHS had occurred long before the
995 DNA collection with the result that the majority of dementia events in the FHS (although
996 ascertained prospectively) were prevalent at the time of DNA collection or these persons had
997 died prior to DNA draw and were thus excluded from analyses of incident disease. Due to the
998 limited number of incident dementia and AD events in the Framingham Offspring only the
999 Original cohort were included in our analyses of incident events.

1000

1001 Rotterdam Study: The Rotterdam Study enrolled inhabitants from a district of Rotterdam
1002 (Ommoord) aged ≥ 55 years ($N=7,983$, virtually all white) at the baseline examination in 1990-93
1003 when blood was drawn for genotyping⁶³. It aims to examine the determinants of disease and
1004 health in the elderly with a focus on neurogeriatric, cardiovascular, bone, and eye disease. All
1005 inhabitants of Ommoord aged ≥ 55 years ($n = 10,275$) were invited and the participation rate was
1006 78%. All participants gave written informed consent to retrieve information from treating
1007 physicians. Baseline measurements were obtained from 1990 to 1993 and consisted of an
1008 interview at home and two visits to the research center for physical examination. Survivors have
1009 been re-examined three times: in 1993-1995, 1997-1999, and 2002-2004. All persons attending
1010 the baseline examination in 1990-93 consented to genotyping and had DNA extracted. This DNA
1011 was genotyped using the Illumina Infinium II HumanHap550chip v3.0[®] array in 2007-2008
1012 according to the manufacturer's protocols. Genotyping was attempted in persons with high-
1013 quality extracted DNA ($n=6,449$). From these 6,449, samples with low call rate ($<97.5\%$, $n=209$),
1014 with excess autosomal heterozygosity (>0.336 , $n=21$), with sex-mismatch ($n=36$), or if there
1015 were outliers identified by the IBS clustering analysis (>3 standard deviations from population
1016 mean, $n=102$ or IBS probabilities $>97\%$, $n=129$) were excluded from the study population with
1017 some persons meeting more than one exclusion criterion; in total, 5,974 samples were available
1018 with good quality genotyping data, 42 persons were excluded since they did not undergo
1019 cognitive screening at baseline, hence their cognitive status was uncertain. An additional 61
1020 persons were excluded because they suffered from dementia other than AD at baseline. After
1021 exclusion of prevalent dementia, a sample of 5752 persons was available. The Rotterdam Study
1022 (including its brain magnetic resonance imaging (MRI) and neurological components) has been
1023 approved by the institutional review board (Medical Ethics Committee) of the Erasmus Medical
1024 Center and the Netherlands Ministry of Health, Welfare and Sports Participants were screened
1025 for prevalent dementia in 1990-93 using a three-stage process; those free of dementia remained
1026 under surveillance for incident dementia, a determination made using records linkage and
1027 assessment at three subsequent re-examinations. We included all prevalent cases and all incident
1028 events up to 31st December 2007.

1029 Screening was done with the MMSE and GMS organic level for all persons. Screen-positives
1030 (MMSE <26 or Geriatric Mental Schedule (GMS) organic level >0) underwent the CAMDEX.
1031 Persons who were suspected of having dementia underwent more extensive neuropsychological

1032 testing. When available, imaging data were used. In addition, all participants have been
1033 continuously monitored for major events (including dementia) through automated linkage of the
1034 study database with digitized medical records from general practitioners, the Regional Institute
1035 for Outpatient Mental Health Care and the municipality. In addition physician files from nursing
1036 homes and general practitioner records of participants who moved out of the Ommoord district
1037 were reviewed twice a year. For suspected dementia events, additional information (including
1038 neuroimaging) was obtained from hospital records and research physicians discussed available
1039 information with a neurologist experienced in dementia diagnosis and research to verify all
1040 diagnoses. Dementia was diagnosed in accordance with internationally accepted criteria for
1041 dementia (Diagnostic and Statistical Manual of Mental Disorders, Revised Third Edition, DSM-
1042 III-R), and AD using the NINCDS-ADRDA criteria for possible, probable and definite AD. The
1043 National Institute of Neurological Disorders and Stroke–Association Internationale pour la
1044 Recherche et l'Enseignement en Neurosciences (NINDS-AIREN) criteria were used to diagnose
1045 vascular dementia. The final diagnosis was determined by a panel of a neurologist,
1046 neurophysiologist, and research physician and the diagnoses of AD and VaD were not mutually
1047 exclusive.

1048 1049 (5) Power Calculation

1050 To determine the power to detect genetic variants associated with age at onset, we ran analyses
1051 using Proc Power in SAS. The analysis was run using minor allele frequencies ranging from 0.05
1052 to 0.50, OR 1.1 to 1.75 and sample size of 45,000. Other factors, such as genetic heterogeneity
1053 and gene-environment interaction are likely to affect these estimates. Alpha was adjusted to
1054 5×10^{-8} . For variants with a MAF of 0.15, we would have approximately 80% power to detect
1055 effects for OR > 1.23 or < 0.81; for variants with a MAF of 0.3, we would have approximately
1056 80% power to detect effects for OR > 1.18 (or < 0.85).

1057 1058 *CSF biomarker datasets*

1059 CSF samples were obtained from the Knight-ADRC (N=805), ADNI-1 (N=390), ADNI-2
1060 (N=397), the Biomarkers for Older Controls at Risk for Dementia (BIOCARD) (N=184), Mayo
1061 Clinic (N=433), Lund University (Swedish) (N=293), University of Pennsylvania (Penn)
1062 (N=164), University of Washington (N=375), The Parkinson's Progression Markers Initiative
1063 (500) and Saarland University (German) (N=105).

1064
1065 Cases were diagnosed with dementia of the Alzheimer's type (DAT) according to the NINCDS-
1066 ADRDA²⁰. Control individuals were evaluated using the same criteria and showed no symptoms
1067 of cognitive impairment. All participants provided written informed consent and the ethics
1068 committee approved the informed consent procedure (IRB ID #: 201105364). 787 additional
1069 samples with biomarker data used in the analyses were obtained from the ADNI database
1070 (adni.loni.usc.edu). ADNI was launched in 2003 as a public-private partnership, led by Principal
1071 Investigator Michael W. Weiner, MD. The primary goal of ADNI has been to test whether serial
1072 magnetic resonance imaging (MRI), positron emission tomography (PET), other biological
1073 markers, and clinical and neuropsychological assessment can be combined to measure the
1074 progression of mild cognitive impairment (MCI) and early Alzheimer's disease (AD).
1075 CSF in all studies was collected in a standardized manner^{12,64-67}. Biomarker measurements
1076 within each study were conducted using internal standards and controls to achieve consistency
1077 and reliability. However, differences in the measured values between studies were observed

1078 which are likely due to differences in the antibodies and technologies used for quantification
1079 (standard ELISA with Innostest for Knight-ADRC, UW, Swedish, German, and Mayo versus
1080 Luminex with AlzBio3 for ADNI-1, ADNI-2, BIOCARD and Penn), ascertainment and/or
1081 handling of the CSF after collection. CSF A β ₄₂ and ptau₁₈₁ values were log transformed in order
1082 to approximate a normal distribution. Because the CSF biomarker values were measured using
1083 two different platforms (standard ELISA with Innostest and Luminex with AlzBio3), we did not
1084 combine the raw data. For the combined analyses, we standardized the mean of the log-
1085 transformed values from each dataset to zero. No significant differences in the transformed and
1086 standardized CSF values were found between cohorts. We also performed meta-analyses for the
1087 most significant SNPs by combining the P values for each independent dataset using METAL⁶⁸.
1088 No major differences were found between the joint-analyses and the meta-analyses.

1089

1090 *Quality Control*

1091 For survival analysis, we excluded cases with AAO below 60 and cases with prevalent stroke.
1092 For CSF analysis, individuals under age 45 years were removed because prior studies have
1093 demonstrated that the relationship between CSF A β ₄₂ levels and age appears to differ in
1094 individuals below 45 years vs. those above 45 years⁶⁹. Of the remaining individuals in both
1095 analyses, we excluded individuals who had > 5% missing genotype rates, who showed a
1096 discrepancy between reported sex and sex estimated on the basis of genetic data, or who showed
1097 evidence of non-European ancestry based on principal component analysis using PLINK1.9⁷⁰.
1098 We identified unanticipated duplicates and cryptic relatedness using pair-wise genome-wide
1099 estimates of proportion identity by descent (IBD) using PLINK. When duplicate samples or a
1100 pair of samples with cryptic relatedness was identified, the sample with the lower genotyping
1101 call rate was removed. We excluded potentially related individuals so that all remaining
1102 individuals have kinship coefficient below 0.05. Finally, we excluded individuals with missing
1103 disease status, age or gender information.

1104 To control for genotype quality, we excluded SNPs with missing genotypes in > 5% of
1105 individuals in each dataset for survival analysis, and > 2% for CSF association analysis. For the
1106 EADI cohort, variants with minor allele frequency < 1%, Hardy-Weinberg P value < 1x10⁻⁶ and
1107 missingness > 2% were removed prior to imputation. Genome-wide genotype imputation was
1108 performed using IMPUTE2⁷¹ with 1000 Genomes reference haplotypes. We excluded imputed
1109 SNPs with an IMPUTE2 quality score < 0.5 for survival analysis. For CSF association, we
1110 excluded SNPs with an IMPUTE2 quality score of < 0.3 since the dataset was only used for
1111 follow-up. In the ADGC, GERAD, CHARGE, and CSF datasets, we then removed SNPs that
1112 failed the Hardy-Weinberg equilibrium in controls calculated based on the imputed best-guess
1113 genotypes using a P value threshold of 1x10⁻⁶. We excluded SNPs with minor allele frequency \leq
1114 0.02. Finally, we excluded SNPs with available statistics in only one consortium dataset in the
1115 meta-analysis. The number of filtered samples and SNPs in each of the above steps are recorded
1116 in **Supplementary Table 1**.

1117

1118 *Genome-wide survival association study*

1119 We conducted a genome-wide Cox proportional hazards regression⁷² assuming an additive effect
1120 from SNP dosage. The Cox proportional hazard regression was implemented in the R survival
1121 analysis package. We incorporated sex, site and the first three principal components from
1122 EIGENSTRAT³⁰ in all our regression models to control for their effects. For EADI, sex and four
1123 principal components were included in the model. For the Cox model, the time scale is defined

1124 as age in years, where age is age at onset for cases and age at last assessment for controls. The
1125 formula applied is as followed:

$$h(t|X) = h_0(t) \exp\left(\sum_{i=1}^p \beta_i X_i\right)$$

1126 where $X = (X_1, X_2, \dots, X_p)$ are the observed values of covariates for subject i . The Cox model
1127 has previously been shown to be applicable to case-control datasets without an elevated type 1
1128 error rate nor overestimation in effect sizes^{73,74}. The model assumes log-linearity and
1129 proportional hazards. The assumption of log-linearity is common in the additive logistic
1130 regression used in a typical GWAS. We validated the assumption of proportional hazards
1131 assumed by the Cox model by conducting the Schoenfeld test in the 22 prioritized SNPs. None
1132 of the SNPs has a Schoenfeld P value, which is the P value for Pearson product-moment
1133 correlation between the scaled Schoenfeld residuals and time, lower than 0.035 (multiple test
1134 correction threshold = 0.00227) in any of the 7 cohorts. Further, only 3 out of the 148 P values
1135 were less than 0.05, suggesting that the time proportionality assumption is unlikely to be violated
1136 in these associations (**Supplementary Table 1**). Similarly, the Schoenfeld test was conducted for
1137 all 22 SNP association models on the covariates in the ADGC and GERAD cohort
1138 (**Supplementary Table 1**). We also examined the effect sizes of our candidate SNPs in these
1139 cohorts and found consistent effect sizes (**Supplementary Fig. 3**) in the 3 retrospective case-
1140 control cohorts (ADGC, GERAD, EADI case-control) and 4 prospective cohorts (EADI-
1141 prospective, CHARGE FHS, CHS and Rotterdam).
1142 After the analysis of each dataset, we carried out an inverse-variance meta-analysis on the results
1143 using METAL²⁶, applying a genomic control to adjust for inflation in each dataset. Of the 751
1144 suggestive SNPs ($P < 1 \times 10^{-5}$), we found these SNPs to show lower standard errors and
1145 confidence intervals with the increasing number of cohorts showing consistent directionalities of
1146 effect. Particularly, the average standard error for SNPs showing 1 to 7 consistent directionalities
1147 ranges from 0.171, 0.109, 0.0744, 0.0346, 0.0234, 0.0173 to 0.01795 (**Supplementary Fig. 1b**).
1148 Thus, we limited our final analysis to SNPs that showed consistent directionalities of effect in at
1149 least 6 out of the 7 datasets included in the meta-analysis. The association graphs of results from
1150 loci of interest were plotted using LocusZoom⁷⁵.

1151 *CSF biomarker association analysis*

1153 For the CSF datasets, we performed multivariate linear regression for CSF $A\beta_{42}$ and tau, and
1154 ptau_{181} association adjusting for age, gender, site, and the first three principal components using
1155 PLINK.

1156 *eQTL analysis*

1158 We examined the effect of top survival and CSF SNPs on gene expression using published
1159 databases. For general brain expression eQTL analysis, we queried the BRAINEAC eQTL data
1160 provided by the UK human Brain Expression Consortium (see URLs).
1161 We conducted leukocyte-specific analysis using the Cardiogenics dataset²⁷ composed of 738
1162 monocytes and 593 macrophages samples. For each probeset – imputed SNP pair, a simple linear
1163 regression was used to analyze the data separately for monocytes and macrophages:

$$y_i = \alpha + \beta x_i + \varepsilon_i, 1 \leq i \leq n, \varepsilon_i \sim N(0, \sigma^2)$$

1164 where i is the subject index, x is the effective allele copy number, and y_i is the covariates-
1165 adjusted, inverse-normal transformed gene expression. Significance of *cis* (SNP within $\pm 1\text{Mb}$ of

1166 the closest transcript end) eQTL effects were quantified with a Wald test on the ordinary Least
1167 Squares (OLS) estimator of the coefficient β , obtained with R. The distribution of the Wald test P
1168 values under the null hypothesis of no correlation between genotype and gene expression was
1169 estimated by rerunning the same analysis on a null dataset obtained by permuting the expression
1170 samples identifiers. For additional monocyte eQTL analysis, we queried statistics from Fairfax et
1171 al.²⁸ to validate findings in the Cardiogenics dataset.

1172 For conditional analysis, we performed analysis for *SPII* (probe: ILMN_1696463) against all
1173 SNPs within ± 2 Mb from the closest transcript end, by including the following SNPs effective
1174 allele copy numbers as covariates in the linear regression model, one at a time: rs1057233,
1175 rs10838698, rs7928163, rs10838699, rs10838725, rs1377416. Significance was again assessed
1176 with a two-sided Wald test on the OLS estimator of the coefficient β .

1177
1178 *Gene expression analysis in human and mouse brain cell types*

1179 Cell-type specific gene expression in the human and mouse brain was queried from brain RNA-
1180 Seq databases described in Zhang et al.^{29,30} and Bennett et al.³¹ and plotted using custom R
1181 scripts (see URLs). The mouse astrocytes-FACS and astrocytes-immunopanned in mouse were
1182 collapsed into a single astrocyte cell type.

1183
1184 *Epigenetic analysis in human myeloid cell types*

1185 We utilized HaploReg³⁴ to annotate the regulatory element of the significantly associated SNPs
1186 and their tagging SNPs. The myeloid chromatin marks/states and PU.1 ChIP-Seq data at genetic
1187 loci were further examined through the Washington University Epigenome browser⁷⁶ using the
1188 public Roadmap Epigenomics Consortium public tracks hub as well as custom track hubs for
1189 human monocytes and macrophages (hg19) (see URLs).

1190
1191 *Colocalization (coloc and SMR/HEIDI) analyses*

1192 Colocalization analysis of genetic variants associated with AD and myeloid gene expression was
1193 performed using AAOS GWAS SNP and myeloid (monocyte and macrophage) eQTL datasets
1194 from Cardiogenics as inputs. Overlapping SNPs were retained within the hg19 region
1195 chr11:47100000-48100000 for the *SPII/CELF1* locus, chr11:59500000-60500000 for the *MS4A*
1196 locus, and chr1:169300000-170300000 for the *SELL* locus. Colocalization analysis of AD- and
1197 gene expression-associated SNPs was performed using the 'coloc.abf' function in the 'coloc' R
1198 package (v2.3-1). Default settings were used as prior probability of association: 1×10^{-4} for trait 1
1199 (gene expression), 1×10^{-4} for trait 2 (AD) and 1×10^{-5} for both traits. SMR/HEIDI (v0.65) analysis
1200 was performed as described in Zhu et al.²³ and the companion website (see URLs). The ADGC
1201 subset of the IGAP GWAS dataset was used to perform the LD calculations.

1202
1203
1204

1205 *Partitioned heritability analysis using LD score regression*

1206 We used LDSC (LD Score, v1.0.0) regression analysis²⁵ to estimate heritability of AD and
1207 schizophrenia from GWAS summary statistics (excluding the APOE [chr19:45000000-45800000]
1208 and MHC/HLA [chr6:28477797-33448354] regions) partitioned by PU.1 ChIP-Seq binding sites
1209 in myeloid cells, as described in the companion website (see URLs) and controlling for the 53
1210 functional annotation categories of the full baseline model. GWAS summary statistics for AD
1211 and schizophrenia (SCZ) were downloaded from the IGAP consortium¹ (stage 1 dataset) and the

1212 Psychiatric Genomics Consortium (PGC)²⁶ (pgc.cross.scz dataset), respectively (see URLs).
1213 SPI1 (PU.1) bindings sites were downloaded as filtered and merged CHIP-Seq peaks in BED
1214 format from the ReMap database⁷⁷ (GEO:GSE31621, SPI1, blood monocyte and macrophage
1215 datasets³⁵). SPI1 (PU.1) and POLR2AphosphoS5 binding sites were downloaded as broad CHIP-
1216 Seq peaks in BED format from the Encode portal⁷⁸³⁷ (DCC:ENCSR037HRJ; GEO:GSE30567;
1217 HL60 dataset) (see URLs).

1218

1219 *Phagocytosis assay*

1220 BV2 mouse microglial cell line was kindly provided by Marc Diamond (UT Southwestern
1221 Medical Center). BV2 cells were cultured in DMEM (Gibco 11965) supplemented with 5% FBS
1222 (Sigma F4135) and 100 U/ml penicillin-streptomycin (Gibco 15140). Routine testing of cell lines
1223 using MycoAlert PLUS mycoplasma detection kit (Lonza) showed that BV2 cells were negative
1224 for mycoplasma contamination. pcDNA3-FLAG-PU.1 was a gift from Christopher Vakoc⁷⁹
1225 (Addgene plasmid 66974). pGFP-V-RS with either non-targeting shRNA or PU.1-targeting
1226 shRNAs was purchased from OriGene Technologies (TG502008). The pHrodo red zymosan
1227 conjugate bioparticles from Thermo Fisher (P35364) were used to assess phagocytic activity. For
1228 transient transfections, 200,000 cells were seeded in a 24-well plate. On the next day, cells were
1229 washed with PBS (Gibco 14190) and medium was changed to 400 μ l DMEM supplemented with
1230 2% FBS without antibiotic. Transfection mixes of 0.5 μ g pcDNA3 or 0.5 μ g pcDNA3-FLAG-
1231 PU.1 with 0.5 μ g pCMV-GFP for overexpression of mouse PU.1 and 1 μ g pGFP-V-RS-shSCR, -
1232 shA, -shB and -shD for knock-down of mouse PU.1 were prepared with 2 μ l of Lipofectamine
1233 2000, incubated for 20 min at room temperature and added to each well. After 8 hours of
1234 incubation 1 ml of growth medium was added to each well and plates were incubated for 2 days.
1235 Then the medium was replaced with 500 μ l of fresh medium, and 25 μ g of bioparticles were
1236 added to cells for 3 hour incubation. Bioparticles uptake was verified with a fluorescent
1237 microscope; then the cells were collected with trypsin (Gibco #25200), washed with PBS once
1238 and re-suspended in 500 μ l PBS with 1% BSA. Cells were kept on ice and phagocytic activity
1239 was analyzed on an LSR II flow cytometer (BD Biosciences). At least 30,000 events were
1240 collected in each experiment, gated on FSC-A/SSC-A and further on FSC-A/FSC-W dot plot to
1241 analyze populations of viable single cells. Data were quantified using FCS Express 5 (De Novo
1242 Software) and GraphPad Prism 7 (GraphPad Software). Cells pretreated with 2 μ M Cytochalasin
1243 D for 30 minutes before and during the uptake of bioparticles were used as a negative control.
1244 The population of GFP⁺/pHrodo⁺ cells in each condition was used to quantify the phagocytic
1245 index: percentage of pHrodo⁺ cells in GFP⁺ gated population x geometric mean pHrodo intensity
1246 / 10⁶; and represented as phagocytic activity. Three independent experiments were performed
1247 with two technical replicates without randomization of sample processing, n = 3. Researcher was
1248 not blinded to the samples identification. Differences between the means of preselected groups
1249 were analyzed with one-way ANOVA and Sidak's post hoc multiple comparisons test between
1250 selected groups, with a single pooled variance. Values of Cytochalasin D-treated cells were
1251 excluded from the statistical analysis. Adjusted P values for each comparison are reported, non-
1252 significant differences are not reported.

1253

1254 *Western blotting*

1255 BV2 cells transiently transfected as described for the phagocytosis assay were collected with
1256 trypsin after 48 hours of incubation, washed with PBS and re-suspended in PBS with 1% BSA.
1257 Cells from the same treatment were pooled and sorted on FACSARIA III (BD Biosciences) into

1258 GFP⁺ and GFP⁻ populations, pelleted at 2,000 rpm and lysed in RIPA buffer (50 mM Tris-HCl
1259 pH 7.4, 150 mM NaCl, 1% NP-40, 0.5% sodium deoxycholate, 0.1% SDS and Complete
1260 protease inhibitor tablets (Roche)) with one freeze-thaw cycle and 1 hour incubation on ice.
1261 Protein concentration was quantified using the BCA kit (Thermo Fisher #23225). Equal amounts
1262 of protein were separated by electrophoresis in Bolt 4 – 12% Bis-Tris Plus gels with MOPS SDS
1263 running buffer and transferred using the iBlot 2 nitrocellulose transfer stack. Membranes were
1264 blocked and probed with antibodies against PU.1 (Cell Signaling #2266) and β -Actin (Sigma
1265 #A5441) in 3% non-fat dry milk in TBS / 0.1% Tween-20 buffer. Secondary antibody staining
1266 was visualized using WesternBright ECL HRP Substrate Kit (Advansta K-12045) and
1267 ChemiDoc XRS+ (BioRad). Images were quantified using ImageJ (NIH) and GraphPad Prism 7
1268 (GraphPad Software). Two independent experiments were performed without randomization of
1269 sample processing, n = 2. Researcher was not blinded to the samples identification. Differences
1270 between every group mean were analyzed with one-way ANOVA and Sidak's post hoc multiple
1271 variance test between selected groups, with a single pooled variance. Adjusted P values for each
1272 comparison are reported.

1273 1274 *Quantitative PCR*

1275 Sorted GFP⁺ BV2 cells after overexpression or knock-down of PU.1 were collected as described
1276 for western blotting. Cell pellets were lysed in QIAzol reagent and RNA was isolated with
1277 RNeasy Mini kit according to the manufacturer's instructions (Qiagen) including the Dnase
1278 treatment step with RNase-free DNase set (Qiagen). Quantities of RNA were measured using
1279 Nanodrop 8000 (Thermo Scientific) and reverse transcription was performed with 1-2 μ g of total
1280 RNA using High-Capacity RNA-to-cDNA kit (Thermo Fisher Scientific). qPCR was performed
1281 on QuantStudio 7 Flex Real-Time PCR System (Thermo Fisher Scientific) using Power SYBR
1282 Green Master Mix (Applied Biosystems) with one-step PCR protocol. 3 ng of cDNA was used
1283 for all genes except *Ms4a4a* when 24 ng of cDNA was used in a 10 μ l reaction volume. Primers
1284 were from PrimerBank⁸⁰ or designed using Primer-BLAST program (NCBI) and are listed in
1285 **Supplementary Table 14**. Ct values were averaged from two technical replicates for each gene.
1286 Geometric mean of average Ct for the housekeeping genes *GAPDH*, *B2M* and *ACTB* was used as
1287 a reference that was subtracted from the average Ct for a gene of interest (dCt). Gene expression
1288 levels were log transformed (2^{-dCt}) and related to the combined mean values of pcDNA3 and
1289 pGFP-V-RS-shSCR control samples in each sort giving relative expression for each gene of
1290 interest. Data were visualized in GraphPad Prism 7 (GraphPad Software). Four independent
1291 experiments were performed without randomization of sample processing, n = 4. Researcher was
1292 not blinded to the sample identity. Differences between means were analyzed using one-way
1293 ANOVA and Dunnett's post hoc multiple comparisons test between experimental and control
1294 groups, with a single pooled variance. Adjusted P values for each comparison are reported in
1295 **Supplementary Table 13**.

1296 1297 *Data availability*

1298 Summary statistics for the genome-wide survival analyses are posted on the NIA Genetics of
1299 Alzheimer's Disease Data Storage (NIAGADS, see URLs).

1300 1301 *Code availability*

1302 Codes for analyses are available at a public GitHub repository
1303 (https://github.com/kuanlinhuang/AD_SPI1_project).

1304 **URLs**

1305 BRAINEAC, <http://caprica.genetics.kcl.ac.uk/BRAINEAC>; LDSC software,
1306 <http://www.github.com/bulik/ldsc>; baseline and cell type group annotations,
1307 <http://data.broadinstitute.org/alkesgroup/LDSCORE/>; stratified LD score regression companion
1308 website, <https://github.com/bulik/ldsc/wiki/Partitioned-Heritability>; SMR/HEIDI software and
1309 companion website, <http://cnsgenomics.com/software/smr>; Brain RNA-Seq,
1310 http://web.stanford.edu/group/barres_lab/brainseq2/brainseq2.html; WashU EpiGenome Browser,
1311 <http://epigenomegateway.wustl.edu/browser>; custom tracks for human monocytes and
1312 macrophages, http://www.ag-rehli.de/TrackHubs/hub_MOMAC.txt; International Genomics of
1313 Alzheimer's Project (IGAP)
1314 http://web.pasteur-lille.fr/en/recherche/u744/igap/igap_download.php; Psychiatric Genomics
1315 Consortium (PGC) <https://www.med.unc.edu/pgc/results-and-downloads>; ReMap database
1316 <http://tagc.univ-mrs.fr/remap>; Encode portal <https://www.encodeproject.org/>; NIAGADS,
1317 <https://www.niagads.org>.
1318

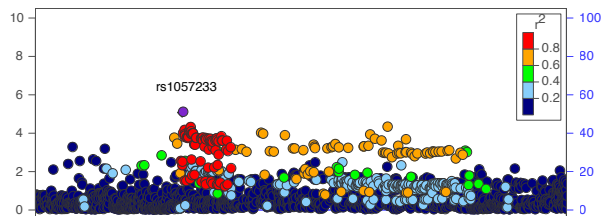
1319 **Methods Reference**

- 1320 51. Alperovitch, A. *et al.* Vascular factors and risk of dementia: Design of the Three-City
1321 Study and baseline characteristics of the study population. *Neuroepidemiology* **22**, 316–
1322 325 (2003).
- 1323 52. Dreses-Werringloer, U. *et al.* A Polymorphism in CALHM1 Influences Ca²⁺
1324 Homeostasis, A β Levels, and Alzheimer's Disease Risk. *Cell* **133**, 1149–1161 (2008).
- 1325 53. Lopez, O. L. *et al.* Evaluation of dementia in the cardiovascular health cognition study.
1326 *Neuroepidemiology* **22**, 1–12 (2003).
- 1327 54. Dawber, T. R. & Kannel, W. B. The Framingham study. An epidemiological approach to
1328 coronary heart disease. *Circulation* **34**, 553–5 (1966).
- 1329 55. Feinleib, M., Kannel, W. B., Garrison, R. J., McNamara, P. M. & Castelli, W. P. The
1330 Framingham offspring study. Design and preliminary data. *Preventive Medicine* **4**, 518–
1331 525 (1975).
- 1332 56. Splansky, G. L. *et al.* The Third Generation Cohort of the National Heart, Lung, and
1333 Blood Institute's Framingham Heart Study: design, recruitment, and initial examination.
1334 *Am. J. Epidemiol.* **165**, 1328–35 (2007).
- 1335 57. Beiser, A., D'Agostino, R. B., Seshadri, S., Sullivan, L. M. & Wolf, P. a. Computing
1336 estimates of incidence, including lifetime risk: Alzheimer's disease in the Framingham
1337 Study. The Practical Incidence Estimators (PIE) macro. *Stat. Med.* **19**, 1495–1522 (2000).
- 1338 58. Bachman, D. L. *et al.* Incidence of dementia and probable Alzheimer's disease in a
1339 general population: the Framingham Study. *Neurology* **43**, 515–519 (1993).
- 1340 59. Farmer, M. E. *et al.* Neuropsychological test performance in Framingham: a descriptive
1341 study. *Psychol. Rep.* **60**, 1023–40 (1987).
- 1342 60. DeCarli, C. *et al.* Measures of brain morphology and infarction in the framingham heart
1343 study: Establishing what is normal. *Neurobiol. Aging* **26**, 491–510 (2005).
- 1344 61. Au, R. *et al.* New norms for a new generation: cognitive performance in the framingham
1345 offspring cohort. *Exp. Aging Res.* **30**, 333–58 (2004).
- 1346 62. Seshadri, S. & Wolf, P. a. Lifetime risk of stroke and dementia: current concepts, and
1347 estimates from the Framingham Study. *Lancet Neurol.* **6**, 1106–1114 (2007).
- 1348 63. Hofman, A. *et al.* The Rotterdam Study: 2014 objectives and design update. *Eur. J.*
1349 *Epidemiol.* **28**, 889–926 (2013).
- 1350 64. Fagan, A. M. *et al.* Inverse relation between in vivo amyloid imaging load and
1351 cerebrospinal fluid A β ₄₂ in humans. *Ann. Neurol.* **59**, 512–519 (2006).
- 1352 65. Peskind, E., Nordberg, A., Darreh-Shori, T. & Soininen, H. Safety of lumbar puncture
1353 procedures in patients with Alzheimer's disease. *Curr. Alzheimer Res.* **6**, 290–292 (2009).

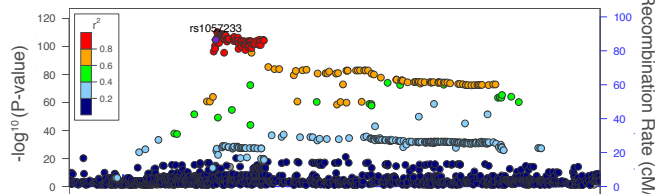
- 1354 66. Grimmer, T. *et al.* Beta Amyloid in Alzheimer's Disease: Increased Deposition in Brain Is
1355 Reflected in Reduced Concentration in Cerebrospinal Fluid. *Biol. Psychiatry* **65**, 927–934
1356 (2009).
- 1357 67. Blennow, K., Hampel, H., Weiner, M. & Zetterberg, H. Cerebrospinal fluid and plasma
1358 biomarkers in Alzheimer disease. *Nat. Rev. Neurol.* **6**, 131–144 (2010).
- 1359 68. Willer, C. J., Li, Y. & Abecasis, G. R. METAL: Fast and efficient meta-analysis of
1360 genomewide association scans. *Bioinformatics* **26**, 2190–2191 (2010).
- 1361 69. Peskind, E. R. *et al.* Age and apolipoprotein E*4 allele effects on cerebrospinal fluid beta-
1362 amyloid 42 in adults with normal cognition. *Arch. Neurol.* **63**, 936–939 (2006).
- 1363 70. Purcell, S. *et al.* PLINK: a tool set for whole-genome association and population-based
1364 linkage analyses. *Am J Hum Genet* **81**, 559–575 (2007).
- 1365 71. Howie, B. N., Donnelly, P. & Marchini, J. A flexible and accurate genotype imputation
1366 method for the next generation of genome-wide association studies. *PLoS Genet.* **5**, (2009).
- 1367 72. Cox, D. R. Regression Models and Life-Tables. *J. R. Stat. Soc. Ser. B-Statistical Methodol.*
1368 **34**, 187–+ (1972).
- 1369 73. Prentice, R. L. & Breslow, N. E. Retrospective Studies and Failure Time Models.
1370 *Biometrika* **65**, 153–158 (1978).
- 1371 74. van der Net, J. B. *et al.* Cox proportional hazards models have more statistical power than
1372 logistic regression models in cross-sectional genetic association studies. *Eur J Hum Genet*
1373 **16**, 1111–1116 (2008).
- 1374 75. Pruim, R. J. *et al.* LocusZoom: Regional visualization of genome-wide association scan
1375 results. *Bioinformatics* **26**, 2336–2337 (2010).
- 1376 76. Zhou, X. *et al.* Exploring long-range genome interactions using the WashU Epigenome
1377 Browser. *Nat. Methods* **10**, 375–6 (2013).
- 1378 77. Griffon, A. *et al.* Integrative analysis of public ChIP-seq experiments reveals a complex
1379 multi-cell regulatory landscape. *Nucleic Acids Res.* **43**, (2015).
- 1380 78. Sloan, C. A. *et al.* ENCODE data at the ENCODE portal. *Nucleic Acids Res.* **44**, D726–
1381 D732 (2016).
- 1382 79. Roe, J. S., Mercan, F., Rivera, K., Pappin, D. J. & Vakoc, C. R. BET Bromodomain
1383 Inhibition Suppresses the Function of Hematopoietic Transcription Factors in Acute
1384 Myeloid Leukemia. *Mol. Cell* **58**, 1028–1039 (2015).
- 1385 80. Wang, X. & Seed, B. A PCR primer bank for quantitative gene expression analysis.
1386 *Nucleic Acids Res.* **31**, e154 (2003).

1387

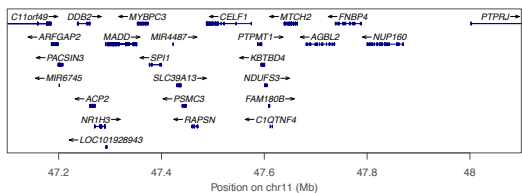
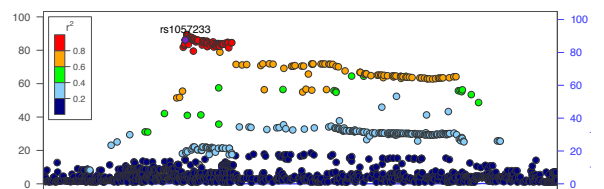
a AD Survival Association



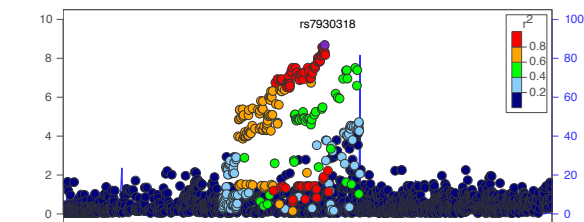
Monocyte *SPI1* eQTL Association (ILMN_1696463)



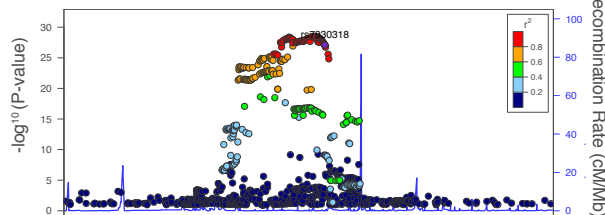
Macrophage *SPI1* eQTL Association (ILMN_1696463)



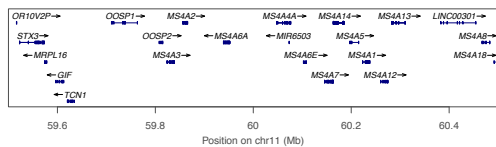
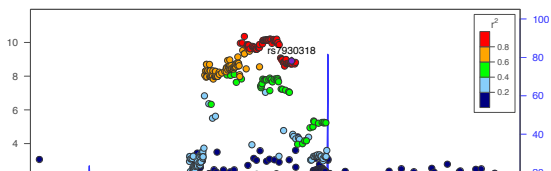
b AD Survival Association

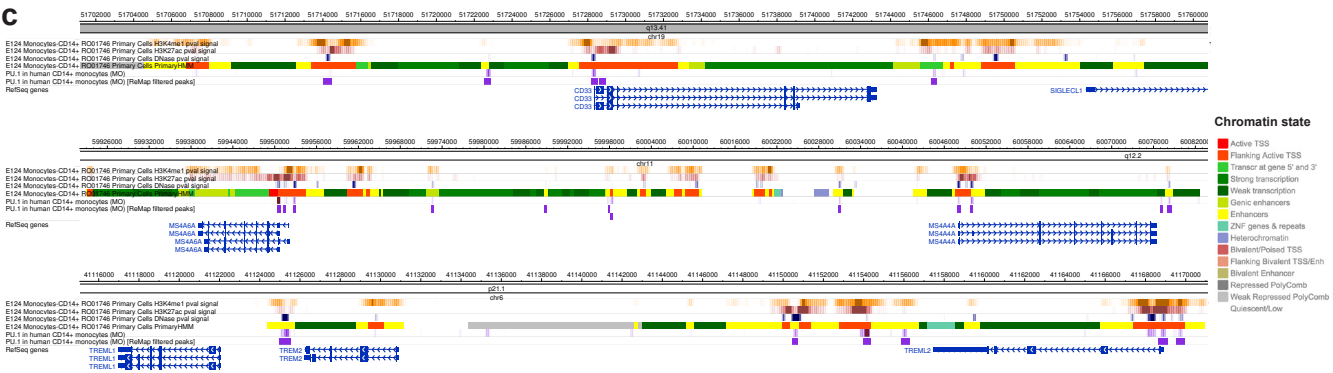
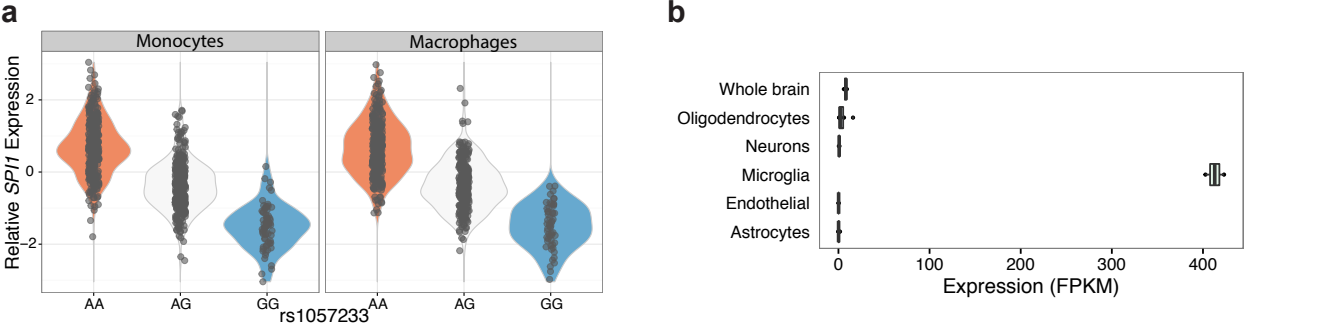


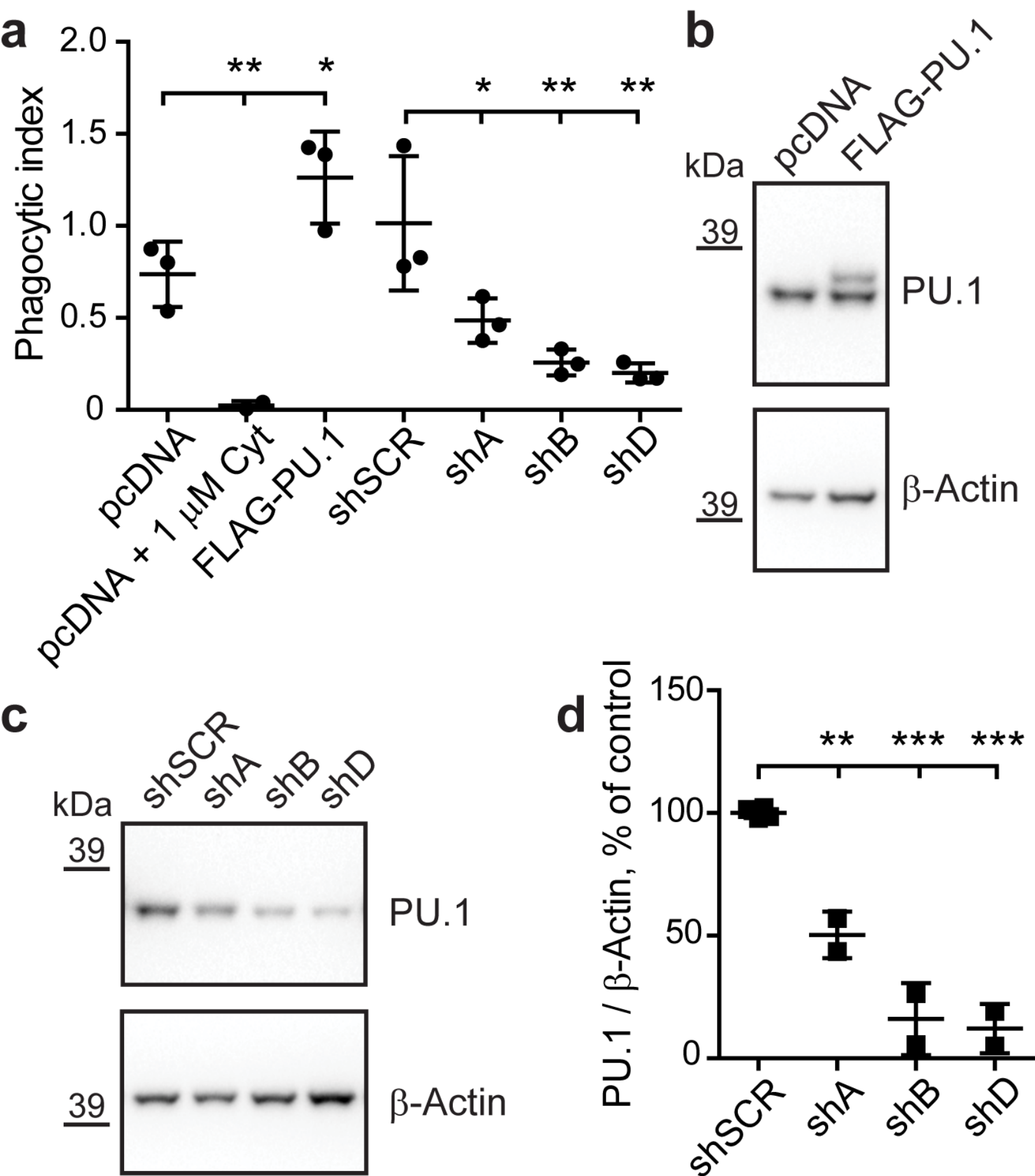
Monocyte *MS4A4A* eQTL Association (ILMN_2370336)

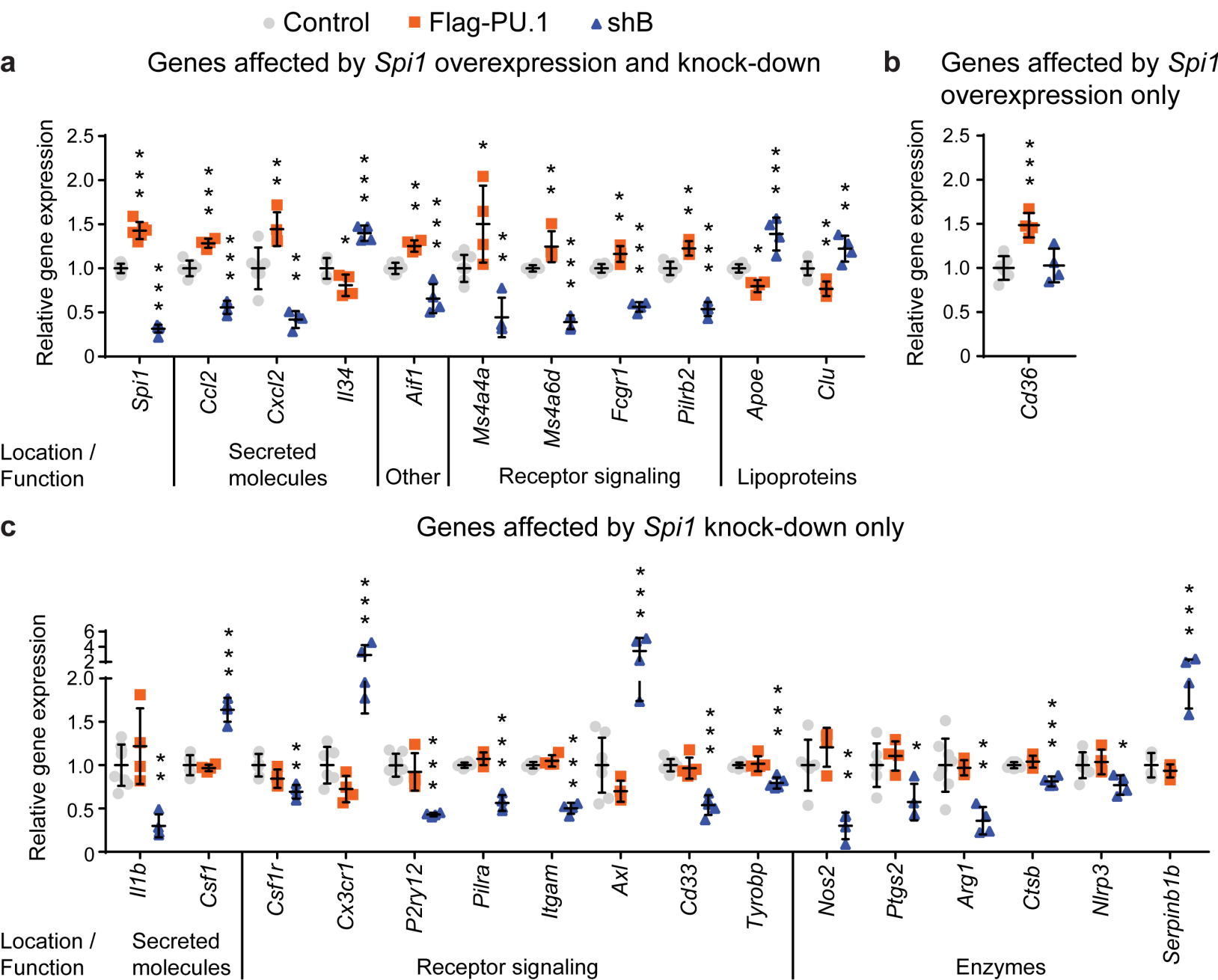


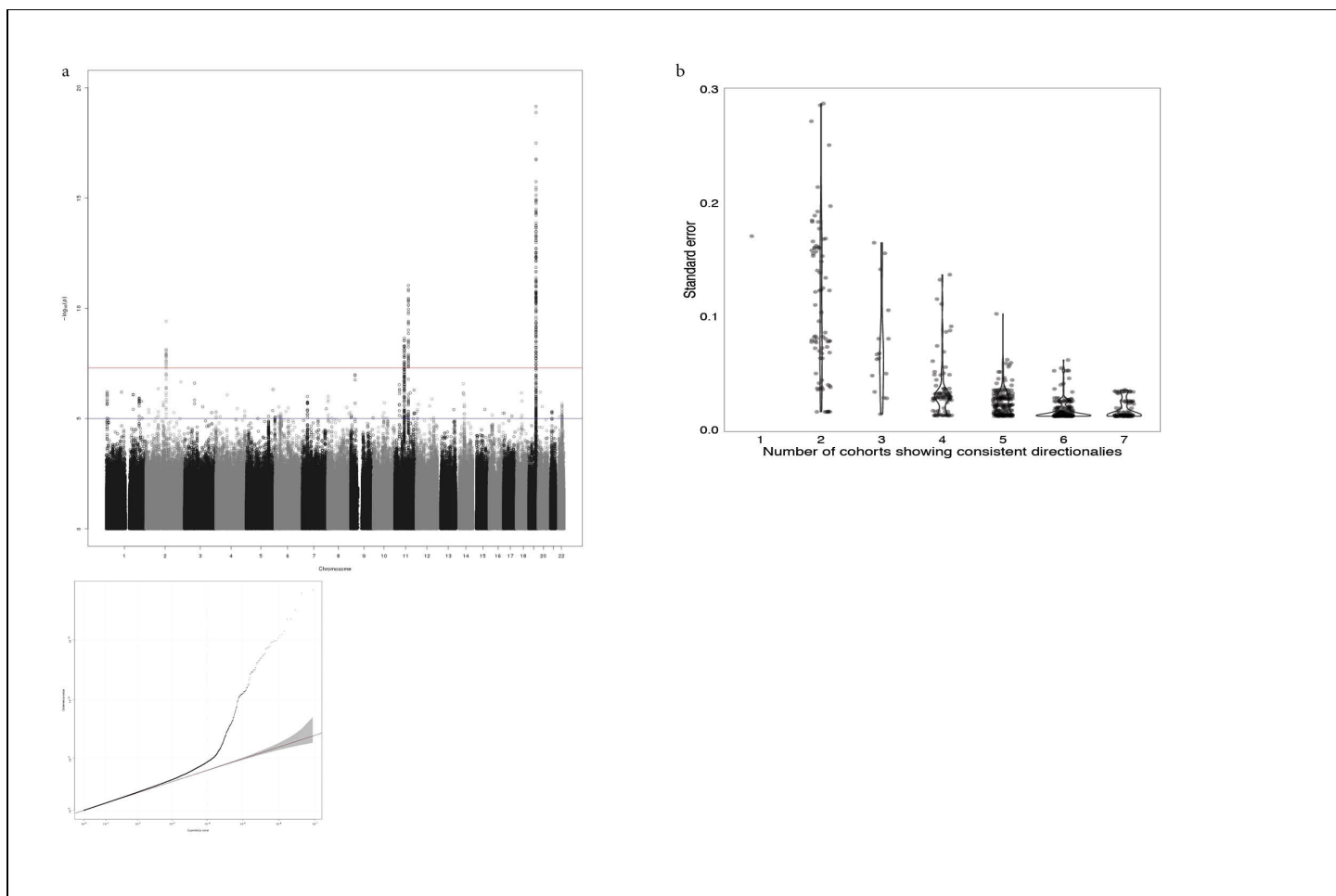
Macrophage *MS4A6A* eQTL Association (ILMN_1721035)







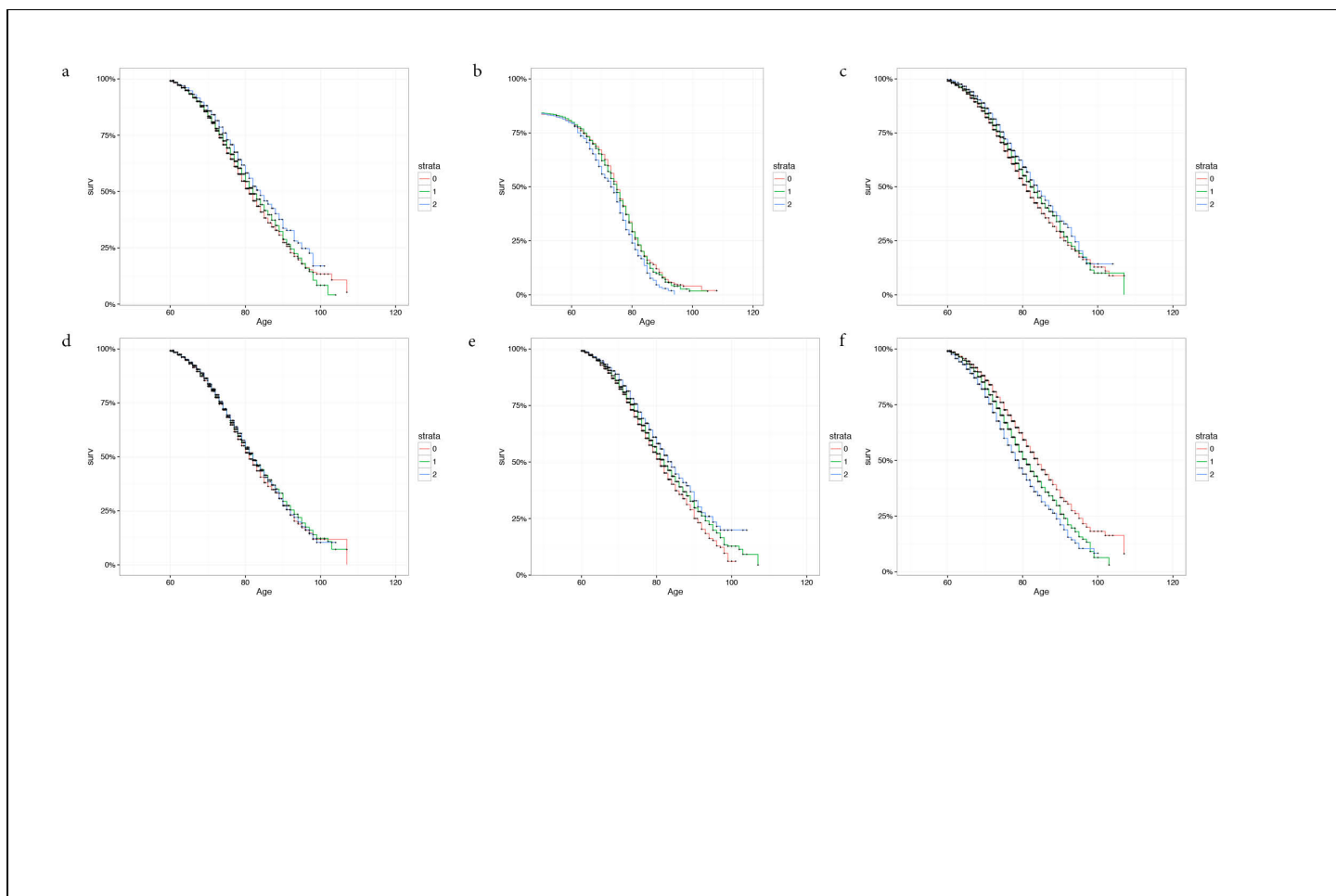




Supplementary Figure 1

Result and quality control analysis of the IGAP AD-survival meta-analysis.

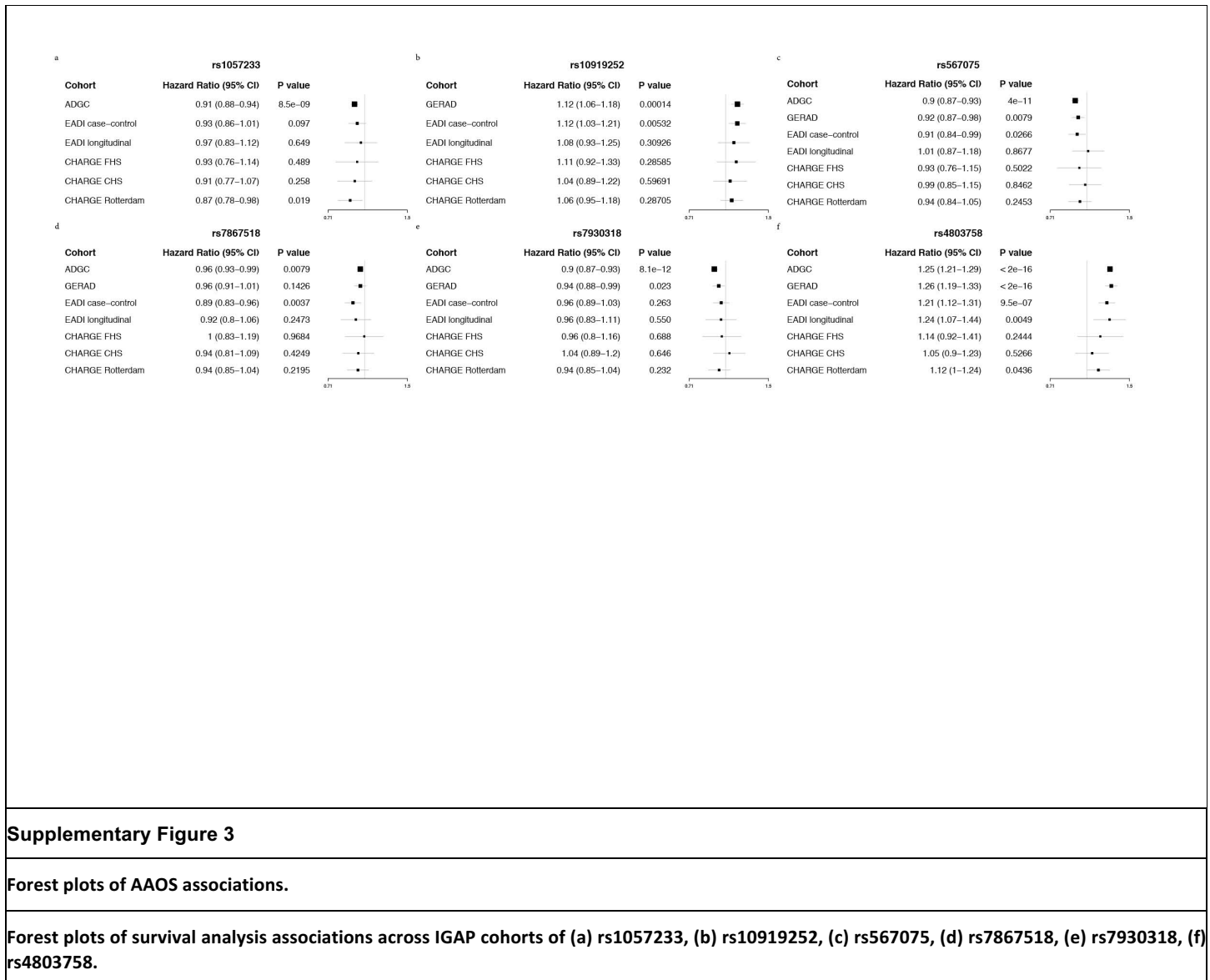
(a) Manhattan plot and QQ-plot of the GWAS. The final meta-analysis showed little evidence of genomic inflation ($\lambda = 1.026$). (b) The average standard error versus the number of cohorts with consistent directionalities of effect sizes.

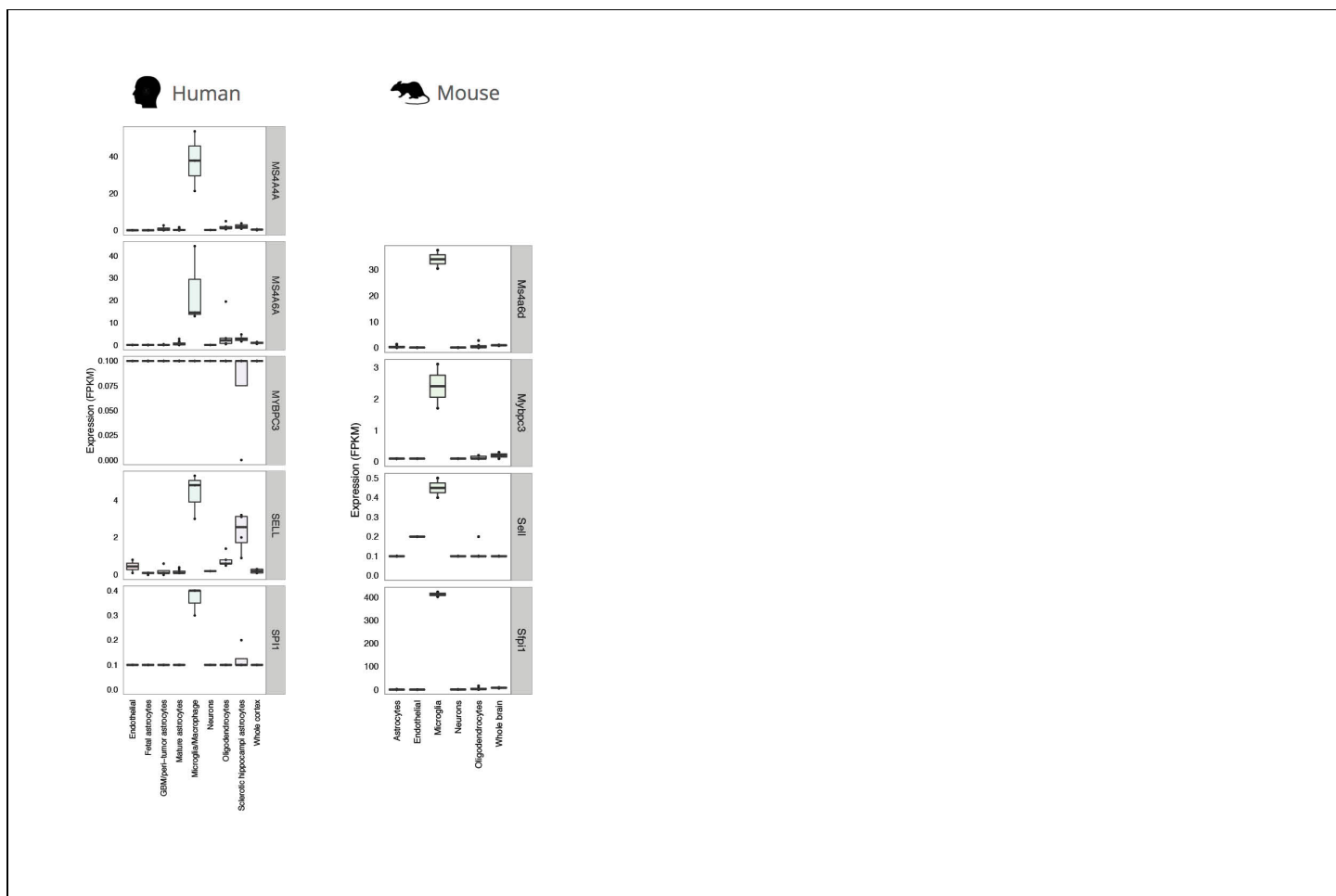


Supplementary Figure 2

Kaplan-Meier plots of AAOs associations.

Kaplan-Meier plots of survival analysis associations in the ADGC cohort of (a) rs1057233, (b) rs10919252, (c) rs567075, (d) rs7867518, (e) rs7930318, (f) rs4803758.

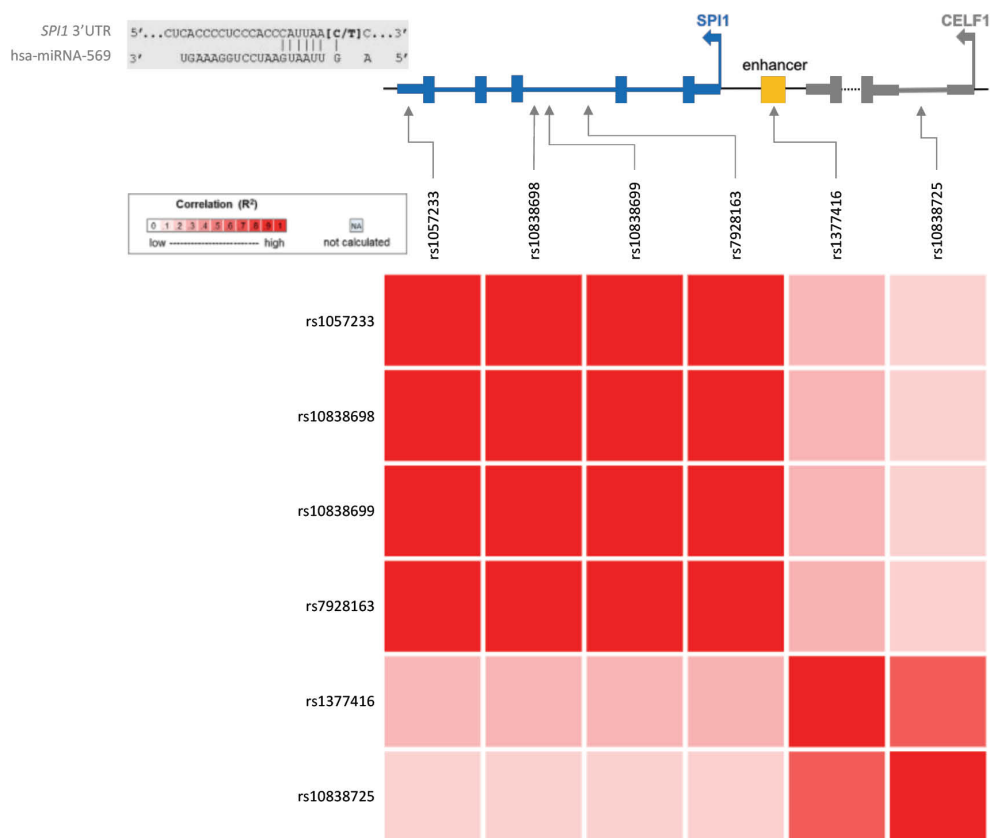




Supplementary Figure 4

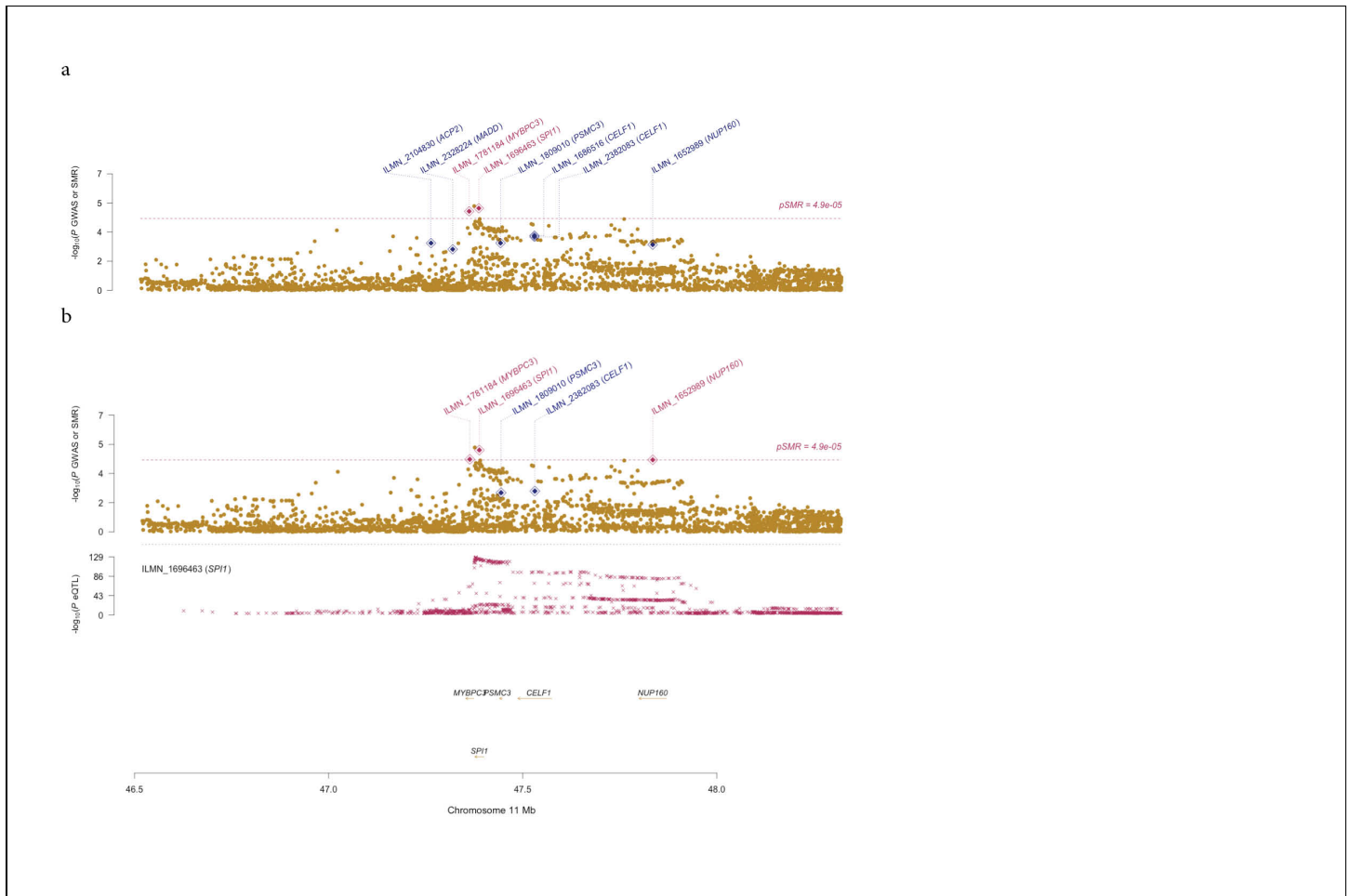
Cell-type specific expression of eQTL-associated genes in brain.

Cell-type specific expression of *MS4A4A* (no mouse homolog available), *SPI1*, *MYBPC3*, *MS4A6A* and *SELL* in human and mouse brains based on the brain RNA-Seq database.



Supplementary Figure 5

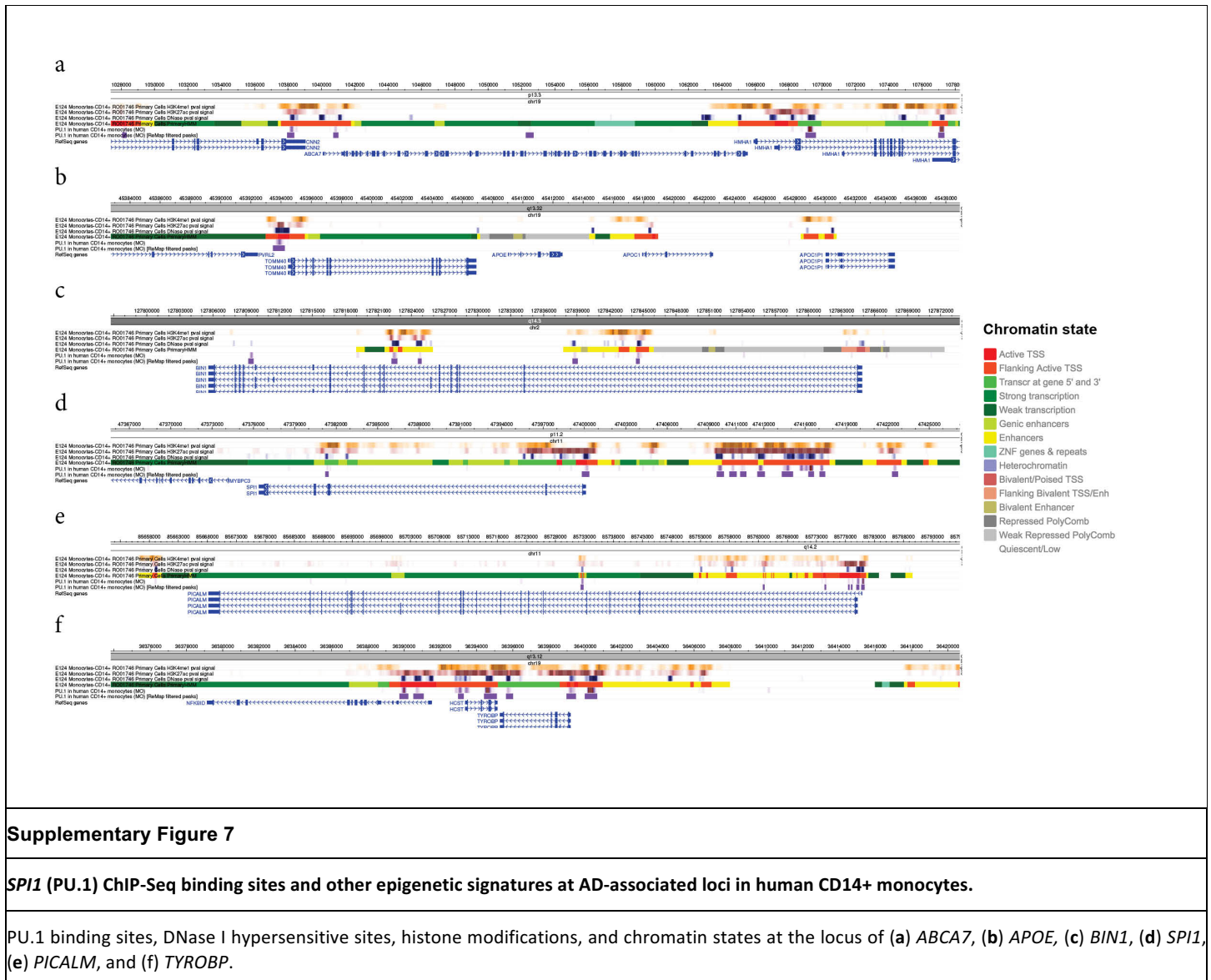
Linkage disequilibrium (LD) plot of SNPs of interest in the *SPI1/CELFI* locus.

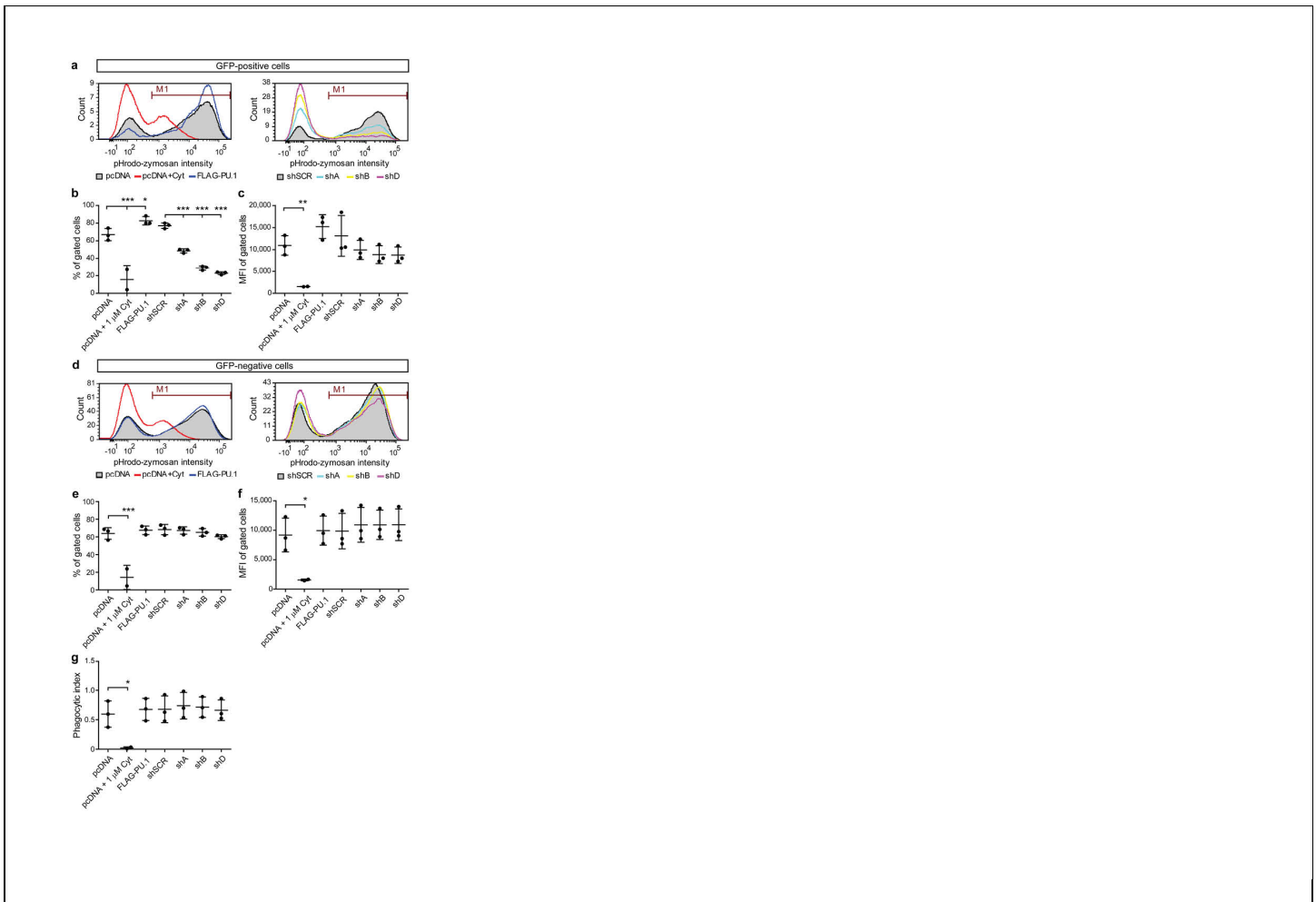


Supplementary Figure 6

SMR plots showing the associations at the *SPI1/CELF1* locus.

SMR plots showing the associations at the *SPI1/CELF1* locus from AAOS GWAS and eQTLs in (a) monocytes and (b) macrophages.

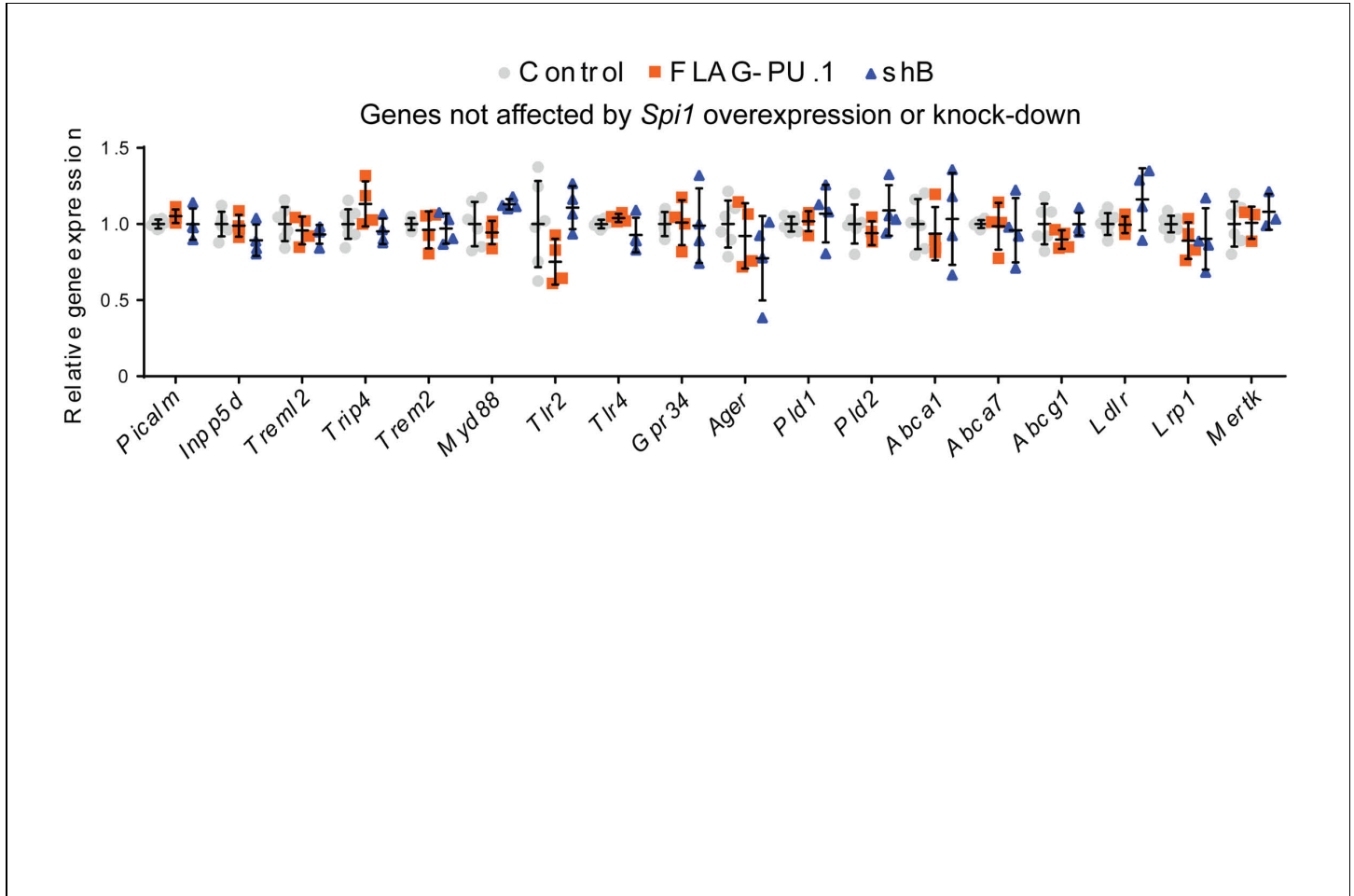




Supplementary Figure 8

Analysis of phagocytosis in BV2 microglial cells.

(a) Flow cytometry histograms of BV2 cells transfected with pcDNA3 (pcDNA) or pcDNA3-FLAG-PU.1 (FLAG-PU.1) with pCMV-GFP for overexpression and scrambled shRNA (shSCR) or PU.1-targeted shRNA (shA, shB and shD) in pGFP-V-RS vector for knock-down of PU.1 after 3 hours of incubation with red pHrodo-labeled zymosan. Cells were gated on GFP+ populations. (b) Flow cytometry analysis of number of gated cells in a presented as mean \pm SD, pcDNA 67.03 \pm 6.883, pcDNA + 1 μ M Cyt 15.64 \pm 16.24, FLAG-PU.1 82.71 \pm 4.74, shSCR 77.17 \pm 3.115, shA 48.63 \pm 2.285, shB 28.92 \pm 2.495, shD 22.76 \pm 1.595. pcDNA vs pcDNA + 1 μ M Cyt $P < 0.0001$, pcDNA vs FLAG-PU.1 $P = 0.0306$, shSCR vs shA $P = 0.0002$, shSCR vs shB $P < 0.0001$, shSCR vs shD $P < 0.0001$. $F(6,13) = 58.68$, $n = 3$. (c) Flow cytometry analysis of geometric mean fluorescent pHrodo intensity in a presented as mean \pm SD, pcDNA 10952 \pm 2206, pcDNA + 1 μ M Cyt 1533 \pm 47, FLAG-PU.1 15226 \pm 2701, shSCR 13129 \pm 4617, shA 9937 \pm 2168, shB 8872 \pm 2019, shD 8754 \pm 1856. pcDNA vs pcDNA + 1 μ M Cyt $P = 0.0092$. $F(6,13) = 6.228$, $n = 3$. (d) Flow cytometry histograms of BV2 cells transfected as in (a) and gated on GFP- populations. (e) Flow cytometry analysis of number of gated cells in d presented as mean \pm SD, pcDNA 63.92 \pm 6.575, pcDNA + 1 μ M Cyt 14.21 \pm 13.66, FLAG-PU.1 67.54 \pm 4.826, shSCR 68.31 \pm 5.784, shA 67.27 \pm 4.144, shB 65.19 \pm 4.268, shD 60.3 \pm 2.181. pcDNA vs pcDNA + 1 μ M Cyt $P < 0.0001$. $F(6,13) = 22.53$, $n = 3$. (f) Flow cytometry analysis of geometric mean fluorescent pHrodo intensity in d presented as mean \pm SD, pcDNA 9186 \pm 2863, pcDNA + 1 μ M Cyt 1545 \pm 147, FLAG-PU.1 9931 \pm 2458, shSCR 9849 \pm 3012, shA 10903 \pm 2949, shB 10912 \pm 2494, shD 10934 \pm 2685. pcDNA vs pcDNA + 1 μ M Cyt $P = 0.0367$. $F(6,13) = 3.473$, $n = 3$. (g) Phagocytic index of BV2 GFP- cells analyzed in (e) and (f) presented as mean \pm SD, pcDNA 0.5954 \pm 0.2223, pcDNA + 1 μ M Cyt 0.0209 \pm 0.0189, FLAG-PU.1 0.6745 \pm 0.188, shSCR 0.6765 \pm 0.2274, shA 0.7382 \pm 0.2255, shB 0.7131 \pm 0.1742, shD 0.6612 \pm 0.1748. pcDNA vs pcDNA + 1 μ M Cyt $P = 0.0331$. $F(6,13) = 3.53$, $n = 3$. Cytochalasin D treatment in all figures was used as a negative control for phagocytosis. * $P < 0.05$, ** $P < 0.01$, *** $P < 0.001$, repeated measures one-way ANOVA with Sidak's post hoc multiple comparisons test.



Supplementary Figure 9

Expression levels of genes related to phagocytosis that were not affected by altered *Spi1* expression.

BV2 cells were transiently transfected with pcDNA3-FLAG-PU.1 and pCMV-GFP or pGFP-v-RS-shB against mPU.1. pcDNA3 and pGFP-V-RS-shSCR were used as controls. RNA was extracted from sorted GFP⁺ cells and used for qPCR validation of expression levels for genes of interest. Values are presented as mean ± SD, n = 4 samples collected independently.